

# Asymptotics of non-intersecting Brownian motions and a $4 \times 4$ Riemann-Hilbert problem

E. Daems, A.B.J. Kuijlaars, and W. Veys <sup>1</sup>

*Department of Mathematics, Katholieke Universiteit Leuven,  
Celestijnenlaan 200 B, 3001 Leuven, Belgium*

evi.daems@wis.kuleuven.be  
arno.kuijlaars@wis.kuleuven.be  
wim.veys@wis.kuleuven.be

## Abstract

We consider  $n$  one-dimensional Brownian motions, such that  $n/2$  Brownian motions start at time  $t = 0$  in the starting point  $a$  and end at time  $t = 1$  in the endpoint  $b$  and the other  $n/2$  Brownian motions start at time  $t = 0$  at the point  $-a$  and end at time  $t = 1$  in the point  $-b$ , conditioned that the  $n$  Brownian paths do not intersect in the whole time interval  $(0, 1)$ . The correlation functions of the positions of the non-intersecting Brownian motions have a determinantal form with a kernel that is expressed in terms of multiple Hermite polynomials of mixed type. We analyze this kernel in the large  $n$  limit for the case  $ab < 1/2$ . We find that the limiting mean density of the positions of the Brownian motions is supported on one or two intervals and that the correlation kernel has the usual scaling limits from random matrix theory, namely the sine kernel in the bulk and the Airy kernel near the edges.

*Keywords:* Multiple orthogonal polynomials, non-intersecting Brownian motion, Riemann-Hilbert problem, steepest descent analysis

---

<sup>1</sup> The first two authors are supported by FWO-Flanders project G.0455.04, by K.U. Leuven research grant OT/04/24, and by the European Science Foundation Program MIS-GAM. The second author is also supported by INTAS Research Network 03-51-6637, and by a grant from the Ministry of Education and Science of Spain, project code MTM2005-08648-C02-01. The third author is supported by FWO-Flanders project G.0318.06.

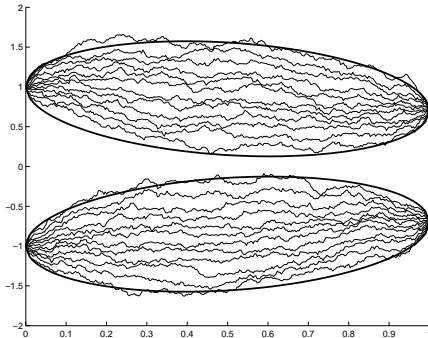


Figure 1: Non-intersecting Brownian motions when  $ab > 1/2$ . Here we have chosen  $a = 1$  and  $b = 0.7$ . For  $ab > 1/2$  we have that the two groups of Brownian motions remain separated during the full time interval  $(0, 1)$ .

## 1 Introduction

Consider  $n$  one-dimensional Brownian motions conditioned not to intersect in the time interval  $(0, 1)$ . We assume that  $n$  is even and that  $n/2$  Brownian motions start at the position  $a > 0$  at time  $t = 0$  and end at  $b > 0$  at time  $t = 1$ , while  $n/2$  Brownian motions start at  $-a$  and end at  $-b$ . If we let  $n \rightarrow \infty$  and at the same time rescale the variance of the Brownian motion with a factor  $1/n$ , then the Brownian motions fill out a region in the  $tx$ -plane that looks like one of the regions shown in Figures 1–3.

The shape of the region depends on the product  $ab$ . For  $ab$  greater than some critical value (which in the units that we will be using is  $1/2$ ) the starting positions  $\pm a$  and the end positions  $\pm b$  are sufficient apart so that the two groups of paths remain separated. The Brownian motions then fill out two ellipses as can be seen in Figure 1. Each group essentially behaves like  $n/2$  non-intersecting Brownian motions with a single starting and end position. This is a variation of Dyson’s Brownian motion for the behavior of the eigenvalues of a Hermitian matrix whose elements evolve according to a Brownian motion [18]. In that model, it holds that at each time  $t \in (0, 1)$  the positions of the paths are distributed like the eigenvalues of a GUE matrix and so follow Wigner’s semi-circle law as  $n \rightarrow \infty$ , see [27]. For the present model and  $ab > 1/2$ , we then also expect to find at each time  $t \in (0, 1)$  the scaling limits for the correlation functions that are known from random matrix theory, and that are expressed in terms of the sine kernel in the bulk, and the Airy kernel at the edge points.

The behavior is different for  $ab$  less than the critical value  $1/2$ . In that case the starting and end positions are not that far apart and the two groups of paths will interact with each other. There are two critical times  $t_{c,1}$  and  $t_{c,2}$  such that the two groups are separated up to the first critical time  $t_{c,1}$ .

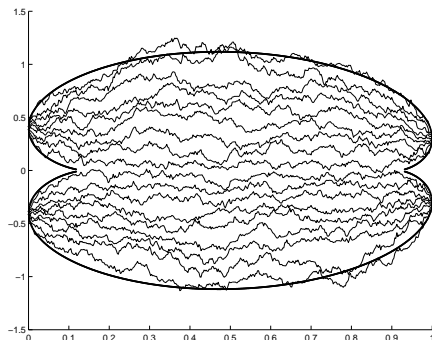


Figure 2: Non-intersecting Brownian motions when  $ab < 1/2$ . Here we have chosen  $a = 0.4$  and  $b = 0.3$ . For  $ab < 1/2$  we have that the two groups of Brownian paths starting at  $\pm a$  come together at the first critical time  $t_{c,1}$ , they merge and continue as one group until the second critical time  $t_{c,2}$ , after which they split again and end at  $\pm b$ .

At  $t_{c,1}$  they merge and continue as one group of paths until the second critical time  $t_{c,2}$  when they split again, see Figure 2. This is an extension of the case of two starting positions and one end position which was studied in [4, 6, 7] with the use of Riemann-Hilbert techniques and in [29] by classical steepest descent techniques. There it was found that for each time  $t \in (0, 1)$ , the scaling limits are still expressed in terms of the sine kernel in the bulk and in terms of the Airy kernel at the edge, except at the cusp point at the critical time. At the cusp the scaling limits are expressed in terms of Pearcey kernels [7, 29] that were first described by Brézin and Hikami [9, 10]. Tracy and Widom [29] also identified a Pearcey process that is further discussed in [1, 2, 25] as well.

Returning to the model with two starting positions and two end positions we have a critical separation  $ab = 1/2$ . Then the starting and end positions have a critical separation so that the two groups of paths just touch in one point, see Figure 3. Here we expect new critical behavior that can be expressed in terms of an as yet unknown kernel.

It is the aim of the present paper to treat the case  $ab < 1/2$ ,  $t \neq t_{c,1}, t_{c,2}$  with the methods of [4, 6, 7]. That is, we use a steepest descent analysis of a relevant Riemann-Hilbert problem that was given by the first two authors in [13]. The Riemann-Hilbert problem has size  $4 \times 4$  and its solution is constructed out of multiple Hermite polynomials of mixed type.

As a result of the asymptotic analysis we find the usual sine kernel in the bulk and the Airy kernel at the edge points, see Theorems 2.2 and 2.3 below, thereby providing further evidence for the universality of these kernels. We are not aware of a double integral representation of the finite  $n$  correlation kernels, so that an asymptotic analysis of integrals as in [29] may not be

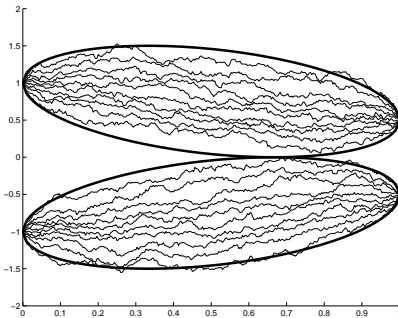


Figure 3: Non-intersecting Brownian motions when  $ab = 1/2$ . Here we have chosen  $a = 1$  and  $b = 1/2$ . For  $ab = 1/2$ , we have that the two groups of Brownian paths touch each other at a critical time  $t_c$ .

possible in this case.

The connections between random matrices and non-intersecting Brownian motions are well-known, see for instance [20] and [30] for a very recent paper on non-intersecting Brownian excursions. Unfortunately we do not know if there exists a corresponding random matrix model for the case studied in this paper.

## 2 Statement of results

### 2.1 Correlation kernel

It follows from the classical paper of Karlin and McGregor [21] that the (random) positions of the Brownian motions at time  $t \in (0, 1)$  are a determinantal point process. This means that there is a kernel  $K_n$  so that for each  $m$  we have that the  $m$ -point correlation function

$$R_m(x_1, \dots, x_m) = \frac{n!}{(n-m)!} \int \dots \int p_{n,t}(x_1, \dots, x_n) dx_{m+1} \dots dx_n,$$

where  $p_{n,t}(x_1, \dots, x_n)$  denotes the joint probability density function for the positions of the paths at time  $t$ , is given by the determinant

$$R_m(x_1, \dots, x_m) = \det(K_n(x_i, x_j))_{i,j=1,\dots,m},$$

see [28].

Indeed, we have by [21] that

$$p_{n,t}(x_1, \dots, x_n) \propto \det(P_n(t, a_j, x_k))_{j,k=1,\dots,n} \det(P_n(1-t, x_k, b_j))_{j,k=1,\dots,n} \quad (2.1)$$

if the non-intersecting paths start at  $a_1 < a_2 < \dots < a_n$  at time  $t = 0$  and end at  $b_1 < b_2 < \dots < b_n$  at time  $t = 1$ , where  $P_n(t, a, x)$  is the transition probability for Brownian motion with variance  $1/n$ ,

$$P_n(t, a, x) = \frac{\sqrt{n}}{\sqrt{2\pi t}} e^{-\frac{n}{2t}(x-a)^2}.$$

Thus (2.1) is a biorthogonal ensemble [8], which is a special case of a determinantal point process. These ensembles are also further studied in connection with random matrix theory in [17]. The correlation kernel is obtained by biorthogonalizing the two sets of functions  $P_n(t, a_j, \cdot)$  and  $P_n(1-t, \cdot, b_j)$  which results in functions  $\phi_j$  and  $\psi_j$  for  $j = 1, \dots, n$ , say, and then putting

$$K_n(x, y) = \sum_{j=1}^n \phi_j(x) \psi_j(y). \quad (2.2)$$

In the situation of the present paper we have to take the confluent limit  $a_j \rightarrow a$ ,  $b_j \rightarrow b$  for  $j = 1, \dots, n/2$ , and  $a_j \rightarrow -a$ ,  $b_j \rightarrow -b$  for  $j = n/2 + 1, \dots, n$ . Then we continue to have a biorthogonal ensemble and the structure of the kernel (2.2) remains the same. In [13] the functions  $\phi_j$  and  $\psi_j$  are written in terms of certain polynomials that were called multiple Hermite polynomials of mixed type. We will use here only the fact that  $K_n$  is expressed in terms of the solution of a Riemann-Hilbert problem, see [13] and (2.16) below.

We assume throughout that

$$0 < ab < 1/2 \quad \text{and} \quad t \in (0, 1) \setminus \{t_{c,1}, t_{c,2}\}. \quad (2.3)$$

So we exclude the critical times from our considerations.

## 2.2 Limiting mean density

Our first result deals with the limiting mean density

$$\rho(x) = \lim_{n \rightarrow \infty} \frac{1}{n} K_n(x, x). \quad (2.4)$$

**Theorem 2.1** *Let  $a, b > 0$  and  $t \in (0, 1)$  such that (2.3) holds. Then the limiting mean density (2.4) of the positions of the Brownian paths at time  $t$  exists. It is supported on one interval  $[-z_1, z_1]$  if  $t \in (t_{c,1}, t_{c,2})$  and on two intervals  $[-z_1, -z_2] \cup [z_2, z_1]$  if  $t \in (0, t_{c,1}) \cup (t_{c,2}, 1)$ . In all cases the density  $\rho(x)$  is expressed as*

$$\rho(x) = \frac{1}{\pi} |\operatorname{Im} \xi(x)|, \quad (2.5)$$

where  $\xi = \xi(x)$  is a solution of the equation

$$\begin{aligned} \xi^4 - \frac{2z}{t(1-t)}\xi^3 + \left( \frac{z^2}{t^2(1-t)^2} - \frac{a^2}{t^2} - \frac{b^2}{(1-t)^2} + \frac{1}{t(1-t)} \right) \xi^2 \\ + \left( \frac{2b^2}{t(1-t)^3} - \frac{1}{t^2(1-t)^2} \right) z\xi - \frac{b^2 z^2}{t^2(1-t)^4} = 0. \end{aligned} \quad (2.6)$$

The density  $\rho$  is real and analytic on the interior of its support and it vanishes like a square root at the edges of its support, i.e., there exists a constant  $c_1$  such that

$$\rho(x) = \frac{c_1}{\pi} |x \mp z_1|^{1/2} (1 + o(1)) \quad \text{as } x \rightarrow \pm z_1, \quad x \in \text{supp } \rho, \quad (2.7)$$

and, in case  $t \in (0, t_{c,1}) \cup (t_{c,2}, 1)$ , there exists a constant  $c_2$  such that

$$\rho(x) = \frac{c_2}{\pi} |x \mp z_2|^{1/2} (1 + o(1)) \quad \text{as } x \rightarrow \pm z_2, \quad x \in \text{supp } \rho. \quad (2.8)$$

### 2.3 Scaling limits of the kernel

As in [4] and [6], the local eigenvalue results are formulated in terms of a rescaled version of the kernel  $K_n$ ,

$$\hat{K}_n(x, y) = e^{n(h(x)-h(y))} K_n(x, y) \quad (2.9)$$

for some function  $h$ . Note that this change in the kernel does not affect the determinants

$$\det(K_n(x_i, x_j))_{1 \leq i, j \leq m}$$

that give the correlation functions for the determinantal process.

Theorems 2.2 and 2.3 show that the kernel has the scaling limits that are universal for unitary ensembles in random matrix theory [15], namely the sine kernel in the bulk, and the Airy kernel at the edge.

**Theorem 2.2** *Let  $a, b > 0$  and  $t \in (0, 1)$  such that (2.3) holds. Let  $z_1, z_2$  be as in Theorem 2.1. Then there exists a function  $h$  such that the following holds for the rescaled kernel (2.9). For every  $x_0 \in (-z_1, z_1)$  (in case  $t \in (t_{c,1}, t_{c,2})$ ) or  $x_0 \in (-z_1, -z_2) \cup (z_2, z_1)$  (in case  $t \in (0, t_{c,1}) \cup (t_{c,2}, 1)$ ) and  $u, v \in \mathbb{R}$ , we have*

$$\lim_{n \rightarrow \infty} \frac{1}{n\rho(x_0)} \hat{K}_n \left( x_0 + \frac{u}{n\rho(x_0)}, x_0 + \frac{v}{n\rho(x_0)} \right) = \frac{\sin \pi(u-v)}{\pi(u-v)}. \quad (2.10)$$

**Theorem 2.3** *Let  $a, b > 0$  and  $t \in (0, 1)$  such that (2.3) holds. Let  $z_1, z_2$  be as in Theorem 2.1. Then there exists a function  $h$  such that the following holds for the rescaled kernel (2.9). For every  $u, v \in \mathbb{R}$ , we have*

$$\begin{aligned} \lim_{n \rightarrow \infty} \frac{1}{(c_1 n)^{2/3}} \hat{K}_n \left( z_1 + \frac{u}{(c_1 n)^{2/3}}, z_1 + \frac{v}{(c_1 n)^{2/3}} \right) \\ = \frac{\text{Ai}(u) \text{Ai}'(v) - \text{Ai}'(u) \text{Ai}(v)}{u - v}, \end{aligned} \quad (2.11)$$

where  $\text{Ai}$  is the usual Airy function, and  $c_1$  is the constant defined in (2.7). In addition, if  $t \in (0, t_{c,1}) \cup (t_{c,2}, 1)$ , then for every  $u, v \in \mathbb{R}$ , we have

$$\begin{aligned} \lim_{n \rightarrow \infty} \frac{1}{(c_2 n)^{2/3}} \hat{K}_n \left( z_2 - \frac{u}{(c_2 n)^{2/3}}, z_2 - \frac{v}{(c_2 n)^{2/3}} \right) \\ = \frac{\text{Ai}(u) \text{Ai}'(v) - \text{Ai}'(u) \text{Ai}(v)}{u - v}, \end{aligned} \quad (2.12)$$

where  $c_2$  is the constant appearing in (2.8).

Similar results hold near  $-z_1$  and  $-z_2$ .

## 2.4 The Riemann-Hilbert problem

Our proofs are based on the fact that the kernel  $K_n$  can be written in terms of the solution of the following Riemann-Hilbert (RH) problem, see [13]. We look for a matrix valued function  $Y : \mathbb{C} \setminus \mathbb{R} \rightarrow \mathbb{C}^{4 \times 4}$  such that

**RH problem for  $Y$**

- (1)  $Y$  is analytic on  $\mathbb{C} \setminus \mathbb{R}$ ,
- (2) for  $x \in \mathbb{R}$ , it holds that

$$Y_+(x) = Y_-(x) \begin{pmatrix} 1 & 0 & w_{1,1}(x)w_{2,1}(x) & w_{1,1}(x)w_{2,2}(x) \\ 0 & 1 & w_{1,2}(x)w_{2,1}(x) & w_{1,2}(x)w_{2,2}(x) \\ 0 & 0 & 1 & 0 \\ 0 & 0 & 0 & 1 \end{pmatrix}, \quad (2.13)$$

where  $Y_+(x)$  ( $Y_-(x)$ ) denotes the limiting value of  $Y(z)$  as  $z$  approaches  $x$  from the upper (lower) half plane,

- (3) as  $z \rightarrow \infty$ , we have that

$$Y(z) = (I + O(1/z)) \begin{pmatrix} z^{n/2} & 0 & 0 & 0 \\ 0 & z^{n/2} & 0 & 0 \\ 0 & 0 & z^{-n/2} & 0 \\ 0 & 0 & 0 & z^{-n/2} \end{pmatrix}. \quad (2.14)$$

In (2.13) we used the functions

$$\begin{aligned} w_{1,1}(x) &= e^{-\frac{n}{2t}(x^2-2ax)}, & w_{1,2}(x) &= e^{-\frac{n}{2t}(x^2+2ax)}, \\ w_{2,1}(x) &= e^{-\frac{n}{2(1-t)}(x^2-2bx)}, & w_{2,2}(x) &= e^{-\frac{n}{2(1-t)}(x^2+2bx)}. \end{aligned} \quad (2.15)$$

This RH problem can be seen as a generalization of the RH problem for multiple orthogonal polynomials [31], which in turn is a generalization of the RH problem for orthogonal polynomials [19].

The kernel  $K_n$  then takes the following form, see [13]:

$$K_n(x, y) = \frac{1}{2\pi i(x-y)} \begin{pmatrix} 0 & 0 & w_{2,1}(y) & w_{2,2}(y) \end{pmatrix} Y_+^{-1}(y) Y_+(x) \begin{pmatrix} w_{1,1}(x) \\ w_{1,2}(x) \\ 0 \\ 0 \end{pmatrix}. \quad (2.16)$$

As explained in [13] the solution of the above RH problem is unique and is built out of polynomials that satisfy certain orthogonality conditions that are a combination of the conditions satisfied by multiple Hermite polynomials of type I and II. Therefore they were called multiple Hermite polynomials of mixed type. The multiple orthogonal polynomials of mixed type and their RH problem are related to multi-component KP as shown in [3].

The formula (2.16) may be seen as a Christoffel-Darboux formula since it equates the sum (2.2) with the right-hand side of (2.16) which is of the form

$$\frac{f_1(x)g_1(y) + f_2(x)g_2(y) + f_3(x)g_3(y) + f_4(x)g_4(y)}{x-y}$$

with only four terms  $f_j(x)g_j(y)$  in the numerator. A similar Christoffel-Darboux formula was derived in [6, 12] for the case of multiple orthogonal polynomials.

We use the Deift/Zhou steepest descent method for Riemann-Hilbert problems and apply it to the Riemann-Hilbert problem stated above. This yields strong and uniform asymptotics for  $Y$  as  $n \rightarrow \infty$  and then also for  $K_n$  due to the formula (2.16).

## 2.5 Riemann surface

As in [4, 6, 7, 23, 26] the asymptotic analysis of the Riemann-Hilbert problem is based on a suitable Riemann surface that in our case is given by the equation (2.6). The determination of the equation for this surface is more complicated in this case, since we could not find an explicit differential equation that is satisfied by the multiple Hermite polynomials of mixed type. We found the equation (2.6) only after numerical experimentation with Maple.



The equation (2.6) has 6 branch points. For  $ab < 1/2$  there are two critical times  $0 < t_{c,1} < t_{c,2} < 1$  such that for  $t_{c,1} < t < t_{c,2}$  four branch points are purely imaginary and two branch points are real, while for  $0 < t < t_{c,1}$  and  $t_{c,2} < t < 1$ , four branch points are real and two branch points are purely imaginary. We prove this in Section 3.3.

The rest of the paper is organized as follows. In Section 3 we give more details about the Riemann surface associated to (2.6) that will be used in the asymptotic analysis of the Riemann-Hilbert problem for  $Y$ , defined in (2.13) and (2.14). In Section 4 we use the Deift/Zhou steepest descent method to analyze this Riemann-Hilbert problem. It leads to the proofs of Theorems 2.1–2.3 in Section 5.

### 3 The Riemann surface

In this section, we study the Riemann surface associated with the equation (2.6) which will be used in Section 4 for the asymptotic analysis of the Riemann-Hilbert problem. When we talk about the Riemann surface we will always mean the compact surface that arises after resolution of the singularities of (2.6).

#### 3.1 Nodal singularities and genus

First of all we note that (2.6) is singular, since clearly both partial derivatives vanish at  $\xi = z = 0$  and so the origin is a singular point. There are also singular points at infinity and to study those it is convenient to introduce homogeneous coordinates  $[z : \xi : w]$  and the homogeneous equation

$$\begin{aligned} \xi^4 - \frac{2}{t(1-t)}z\xi^3 + \frac{1}{t^2(1-t)^2}z^2\xi^2 + \left(-\frac{a^2}{t^2} - \frac{b^2}{(1-t)^2} + \frac{1}{t(1-t)}\right)\xi^2w^2 \\ + \left(\frac{2b^2}{t(1-t)^3} - \frac{1}{t^2(1-t)^2}\right)z\xi w^2 - \frac{b^2}{t^2(1-t)^4}z^2w^2 = 0 \end{aligned} \quad (3.1)$$

in projective space  $\mathbb{P}^2$ .

**Proposition 3.1** *The equation (3.1) has three nodal singularities at  $[0 : 0 : w]$ ,  $[z : 0 : 0]$ , and  $[z : \frac{z}{t(1-t)} : 0]$ . Each of these singularities corresponds to two points on the Riemann surface, and the Riemann surface has genus 0.*

**Proof.** To verify that  $[z : 0 : 0]$  is a node, we set  $z = 1$  in (3.1) and we note that the resulting equation in  $\xi$  and  $w$  has vanishing partial derivatives at  $\xi = w = 0$ . The quadratic part (in  $\xi$  and  $w$ ) is

$$\frac{1}{t^2(1-t)^2}\xi^2 - \frac{b^2}{t^2(1-t)^4}w^2$$

which gives rise to two distinct tangents

$$\xi = \pm \frac{b}{1-t}w \quad (3.2)$$

and therefore  $[z : 0 : 0]$  is a node. Similarly,  $[0 : 0 : w]$  is a node.

The third singularity at  $[z : \frac{z}{t(1-t)} : 0]$  can be readily seen if we rewrite (3.1) as

$$\begin{aligned} \xi^2 \left( \xi - \frac{z}{t(1-t)} \right)^2 - \frac{a^2}{t^2} \xi^2 w^2 + \frac{1}{t(1-t)} \xi w^2 \left( \xi - \frac{z}{t(1-t)} \right) \\ - \frac{b^2}{(1-t)^2} w^2 \left( \xi - \frac{z}{t(1-t)} \right)^2 = 0 \end{aligned} \quad (3.3)$$

Then replacing  $z$  by  $u = \xi - \frac{z}{t(1-t)}$ , setting  $\xi = 1$  and taking the quadratic part (in  $w$  and  $u$ ) we get  $u^2 - \frac{a^2}{t^2} w^2$  which again gives two distinct tangents  $u = \pm \frac{a}{t} w$ . Therefore  $[z : \frac{z}{t(1-t)} : 0]$  is a node as well.

After resolution each of the three nodes leads to two points on the Riemann surface.

The genus formula (Plücker's formula [24, Proposition 2.15]) says that

$$g = (d-1)(d-2)/2 - k$$

for the genus  $g$  of a surface of degree  $d$  with  $k$  nodes and no other singularities. In the present case we have  $d = 4$  and  $k \geq 3$ . Since  $(d-1)(d-2)/2 - k$  is always an upper bound for the genus, we conclude that the Riemann surface has genus zero. We also conclude that there are no other singularities besides the three nodal singularities we already found.  $\square$

### 3.2 Rational parametrization

We find a rational parametrization of the Riemann surface by intersecting the conic

$$\xi^2 - \frac{1}{t(1-t)} z \xi + p \xi w + q z w = 0 \quad (3.4)$$

with the equation (3.1). By Bézout's theorem there are 8 intersection points in  $\mathbb{P}^2$  if we count intersections according to their multiplicities. It is easy to see that the conic intersects equation (3.1) at the three nodes  $[0 : 0 : w]$ ,  $[z : 0 : 0]$ , and  $[z : \frac{z}{t(1-t)} : 0]$  (see Proposition 3.1) for any choice of parameters  $p$  and  $q$ . This accounts for at least 6 intersection points, since each of the nodes counts at least twice. If we choose

$$q = \frac{b}{t(1-t)^2}$$

then the tangent of (3.4) at  $[z : 0 : 0]$  coincides with one of the tangents (3.2). Then we have higher order intersection at  $[z : 0 : 0]$ , so that we have to count this node three times. Then we already have 7 intersection points. The remaining intersection point is a point on the surface that is in one-to-one correspondence with the parameter  $p$  and this gives us the desired parametrization.

Taking  $v = t \left( p + \frac{b}{1-t} \right)$  as a new parameter, we find after simple calculation that

$$\xi = \frac{bv^2 - v + a^2b}{(1-t)(a^2 - v^2)} \quad (3.5)$$

$$\begin{aligned} z &= t(1-t) \left[ \xi + \frac{v\xi}{t\left(\xi - \frac{b}{1-t}\right)} \right] \\ &= \frac{(bv^2 - v + a^2b)((1-t)v^2 - 2tbv + t - (1-t)a^2)}{(2bv - 1)(v^2 - a^2)}. \end{aligned} \quad (3.6)$$

The equations (3.5) and (3.6) parametrize the surface. They give a bijection with the Riemann sphere in the  $v$ -variable and we conclude once again that the surface has genus zero.

### 3.3 The branch points

Now we start to view (2.6) as a four-sheeted branched covering of the Riemann sphere. That is, for each  $z$  the equation (2.6) has four solutions for  $\xi$  where as always we count according to multiplicity. So each  $z$  gives rise to four points or less on the Riemann surface. The branch points correspond to values of  $z$  for which there are at most three points on the Riemann surface. The critical  $t$ -values

$$t_{c,1} = \frac{1 + 2a^2 - \sqrt{1 - 4a^2b^2}}{2(1 + a^2 + b^2)}, \quad t_{c,2} = \frac{1 + 2a^2 + \sqrt{1 - 4a^2b^2}}{2(1 + a^2 + b^2)} \quad (3.7)$$

are such that

$$a^2(1-t)^2 + b^2t^2 = t(1-t). \quad (3.8)$$

In that case, when we put  $z = 0$  in (2.6) we obtain  $\xi^4 = 0$ , which means that the two points on the Riemann surface that correspond to  $z = \xi = 0$  are both branch points. This is the critical case and we will not consider it any further. It is easy to see that for  $ab < 1/2$ , we have  $0 < t_{c,1} < t_{c,2} < 1$ .

The branch points can be found by calculating the zeros of the discriminant of (2.6). With the aid of Maple, we get the following equation for the discriminant:

$$(a_3z^6 + a_2z^4 + a_1z^2 + a_0)z^2 = 0, \quad (3.9)$$

where

$$a_3 = 16a^2b^2, \quad (3.10)$$

$$a_2 = (-48a^2b^2(a-b)^2 + a^4 + b^4)t^2 + (96a^2(a^2 - b^2) - 8a^2)t - 48a^4b^2 - 4a^2, \quad (3.11)$$

$$a_1 = (48a^2b^2(a^4 + b^4 - 7a^2b^2 - a^2 - b^2) + 104a^2b^2 - 8a^4 - 8b^4 + 20a^2 + 20b^2 + 1)t^4 + (48a^2b^2(4a^4 + 14a^2b^2 + 3a^2 + b^2) + 32a^4 - 208a^2b^2 - 60a^2 - 20b^2 - 2)t^3 + (48a^2b^2(6a^4 - 7a^2b^2 - 3a^2) + 104a^2b^2 - 48a^4 + 60a^2 + 1)t^2 + (48a^4b^2(-4a^2 + 1) + 32a^4 - 20a^2)t + 48a^6b^2 - 8a^4, \quad (3.12)$$

$$a_0 = 4(1 - 4a^2b^2)(a^2(1-t)^2 + b^2t^2 - t(1-t))^3. \quad (3.13)$$

Note that  $z = 0$  is always a zero of the discriminant (3.9), but since  $z = \xi = 0$  is a node, this is not a branch point in case  $t \neq t_{c,1}$  and  $t \neq t_{c,2}$ . So (3.9) leads to the sixth degree equation

$$a_3z^6 + a_2z^4 + a_1z^2 + a_0 = 0, \quad (3.14)$$

which has six roots.

We show the following:

**Lemma 3.2** *For every  $t \in (0, 1)$ , the equation (3.14) has only real or purely imaginary roots.*

- (a) *For  $t \in (0, t_{c,1}) \cup (t_{c,2}, 0)$ , there are four real roots  $\pm z_1$  and  $\pm z_2$  with  $z_1 > z_2 > 0$  and two imaginary roots  $\pm iz_3$  with  $z_3 > 0$ .*
- (b) *For  $t \in (t_{c,1}, t_{c,2})$ , there are two real roots  $\pm z_1$  with  $z_1 > 0$  and four purely imaginary roots  $\pm iz_2$  and  $\pm iz_3$  with  $z_3 \geq z_2 > 0$ .*

**Proof.** Because (3.14) only has even powers of  $z$ , it is enough to prove that the polynomial

$$p_1(x) = a_3x^3 + a_2x^2 + a_1x + a_0 \quad (3.15)$$

has three real roots with one negative root and two positive roots in case (a) and one positive root and two negative roots in case (b).

We first examine when (3.15) has a multiple root. We find those values by looking at the zeros of the discriminant of (3.15), which is a polynomial of degree 12 in  $t$ , given by

$$16t(1-t)((a+b)t-a)^2((a-b)t-a)^2 \times ((432a^4b^4 + 8a^2 - 72a^2b^2 - 1 + 8b^2)t^2 + ((-432a^4b^4 + 72a^2b^2 + 1)t(1-t) + 8a^2(1-t)^2 + 8b^2t^2)^3, \quad (3.16)$$

which was calculated with the use of Maple. We find multiple roots for  $t_1 = 0$ ,  $t_2 = 1$ ,  $t_3 = \frac{a}{a+b}$ ,  $t_4 = \frac{a}{a-b}$ , and for the zeros  $t_5$  and  $t_6$  of the quadratic polynomial

$$q(t) = (-432a^4b^4 + 72a^2b^2 + 1)t(1-t) + 8a^2(1-t)^2 + 8b^2t^2.$$

Now it is easy to verify that

$$8a^2\frac{1-t}{t} + 8b^2\frac{t}{1-t}$$

takes its minimum for  $t \in (0, 1)$  in  $t = t_3 = \frac{a}{a+b}$  and the minimum is  $16ab$ . Thus for  $t \in (0, 1)$ ,

$$\begin{aligned} q(t) &\geq t(1-t)(-432a^4b^4 + 72a^2b^2 + 1 + 16ab) \\ &= t(1-t)(1-2ab)(1+6ab)^3 > 0, \end{aligned}$$

since  $ab < 1/2$ . So  $t_5$  and  $t_6$  do not belong to the interval  $(0, 1)$  and the only value of  $t \in (0, 1)$  for which (3.15) has a multiple root is  $t_3 = \frac{a}{a+b}$ . For  $t_3$  we find that  $p_1$  has the following roots:

$$x_1 = \frac{4ab(2ab+1)}{(a+b)^2} \quad \text{and} \quad x_2 = x_3 = -\frac{(2ab-1)^2}{4(a+b)^2}.$$

So for  $t = t_3$  we have that  $p_1$  has a double negative root and one positive root.

Next, we investigate the critical  $t$ -values  $t = t_{c,1}$  and  $t = t_{c,2}$ , see (3.7), which are exactly those  $t \in (0, 1)$  for which  $a_0 = 0$ . So for these values, one root of (3.15) is at  $x = 0$ . We determine the sign of the other two roots by looking at  $a_1$ . We are going to take  $t = t_{c,1}$ . The proof for  $t = t_{c,2}$  is similar. If we substitute  $t = t_{c,1}$  into (3.12), we arrive at the expression

$$\begin{aligned} a_1 = -\frac{27(1-4a^2b^2)^2}{2(a^2+b^2+1)^4} &\left( a^4((4b^2+1)(1+\sqrt{1-4a^2b^2})-2a^2b^2) \right. \\ &\left. + b^4((4a^2+1)(1-\sqrt{1-4a^2b^2})-2a^2b^2) + 12a^4b^4 \right) \end{aligned} \quad (3.17)$$

Since  $0 < ab < 1/2$ , it is easy to check that  $2a^2b^2 < 1 - \sqrt{1-4a^2b^2}$ . Then it readily follows that  $a_1 < 0$  because of (3.17). Thus for  $t = t_{c,1}$  the polynomial  $p_1$  has one negative root, one positive root, and one root at 0. The same holds for  $t = t_{c,2}$ .

Now we can finish the proof of the lemma by a continuity argument. For  $t = t_{c,1}$  and for  $t = t_{c,2}$  we have three distinct real roots. Since there are only multiple roots for  $t = a/(a+b)$  we find three distinct real roots for every  $t$  in the two intervals  $(0, a/(a+b))$  and  $(a/(a+b), 1)$ . Note that  $t_{c,1} < a/(a+b) < t_{c,2}$ .

Since we have a double negative root and one positive root for  $t = a/(a+b)$ , and 0 is only a root for  $t_{c,1}$  and  $t_{c,2}$ , it follows that  $p_1$  has two negative roots and one positive root for every  $t \in (t_{c,1}, t_{c,2})$ .

For  $t = 0$ , we find  $p_1(x) = 4a^2(x - a^2)^2(4b^2x - 4a^2b^2 + 1)$  with roots  $x_1 = x_2 = a^2 > 0$  and  $x_3 = \frac{4a^2b^2 - 1}{4b^2} < 0$ . Then by continuity we find that there are two positive roots and one negative root for every  $t \in (0, t_{c,1})$ . We find the same thing for  $t \in (t_{c,2}, 1)$  by looking at  $t = 1$ .

This completes the proof of the lemma.  $\square$

The six roots of (3.14) are all simple branch points of the Riemann surface. This follows from the Riemann-Hurwitz formula [24, Theorem 4.16], and the fact that the genus is zero.

### 3.4 Sheet structure

There are four inverse functions of (2.6), which behave near infinity as

$$\xi_1(z) = \frac{z}{t(1-t)} - \frac{a}{t} - \frac{1}{2z} + O\left(\frac{1}{z^2}\right), \quad (3.18)$$

$$\xi_2(z) = \frac{z}{t(1-t)} + \frac{a}{t} - \frac{1}{2z} + O\left(\frac{1}{z^2}\right), \quad (3.19)$$

$$\xi_3(z) = \frac{b}{1-t} + \frac{1}{2z} + O\left(\frac{1}{z^2}\right), \quad (3.20)$$

$$\xi_4(z) = -\frac{b}{1-t} + \frac{1}{2z} + O\left(\frac{1}{z^2}\right). \quad (3.21)$$

The sheet structure of the Riemann surface is determined by the way we choose the analytical continuations of the  $\xi$ -functions. Since all branch points are on the real or imaginary axis, we find that all  $\xi_j$ 's have an analytic extension to  $\mathbb{C} \setminus C$  where  $C$  is the cross

$$C = [-z_1, z_1] \cup [-iz_3, iz_3].$$

The analytic continuation is also denoted by  $\xi_j$ . We consider  $\xi_j$  on the  $j$ th sheet.

Now we use the rational parametrization (3.5)–(3.6) of the surface to compute the corresponding curves in the  $v$ -plane. We denote the  $v$ -value corresponding to  $z \in \mathbb{C} \setminus C$  on the  $j$ th sheet by  $v_j(z)$  and we let  $\omega_j$  be the image set of  $v_j(\mathbb{C} \setminus C)$ . The next two figures show the regions  $\omega_j$ ,  $j = 1, 2, 3, 4$ , for the cases  $t < t_{c,1}$  and  $t_{c,1} < t < t_{c,2}$ , respectively. Denoting the point at infinity on the  $j$ th sheet by  $\infty_j$ , we can determine the corresponding  $v$ -values from the formulas (3.5), (3.6), and (3.18)–(3.21). Indeed we have

$$\left\{ \begin{array}{l} z = \infty_1 \longleftrightarrow v = a, \\ z = \infty_2 \longleftrightarrow v = -a, \\ z = \infty_3 \longleftrightarrow v = \frac{1}{2b}, \\ z = \infty_4 \longleftrightarrow v = \infty. \end{array} \right. \quad (3.22)$$

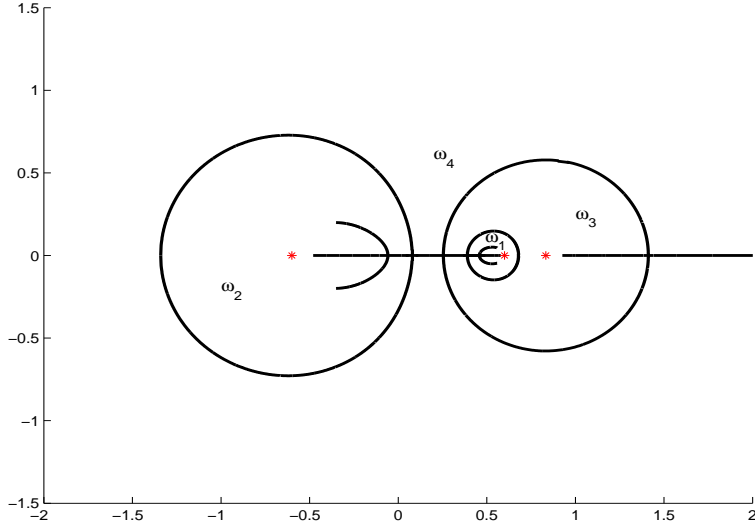


Figure 4: The image of the cross  $C = [-z_1, z_1] \cup [-iz_3, iz_3]$  in the  $v$ -plane for  $0 < t < t_{c,1}$ . The values  $v = -a$ ,  $v = a$ , and  $v = \frac{1}{2b}$  are indicated with  $*$ . These  $v$ -values correspond to  $\infty$  on the second, first and third sheets, respectively. The precise values used for the figure are  $a = b = 0.6$  and  $t = 0.25$ .

These four  $v$ -values are independent of  $t$ , and they are indicated with  $*$  in Figures 4 and 5 (except for  $v = \infty$ , which is of course not visible). Note that  $-a < a < \frac{1}{2b}$ .

The figures show what the analytic continuations are of the functions  $\xi_j$  and how the sheets of the Riemann surface are connected. First of all, we note that any part of the boundary of  $\omega_j$  that is not a part of the boundary of some  $\omega_k$  with  $k \neq j$ , corresponds in the  $z$ -plane to a part of the cross  $C$  where  $\xi_j$  has equal boundary values from both sides. This part of the cross is then removed from the cut on the  $j$ th sheet.

In this way, we see that for  $t < t_{c,1}$ ,  $\xi_1$  is defined with a cut  $[z_2, z_1]$  only,  $\xi_2$  with a cut  $[-z_1, -z_2]$ ,  $\xi_3$  with two cuts  $[z_2, z_1]$  and  $[-iz_3, iz_3]$  and  $\xi_4$  is defined with two cuts  $[-z_2, -z_1]$  and  $[-iz_3, iz_3]$ . The sheets are connected as shown in Figure 6.

For  $t_{c,1} < t < t_{c,2}$  we have the two pairs of purely imaginary branch points  $\pm iz_2$  and  $\pm iz_3$ , where we choose  $z_3 \geq z_2$ . In the situation of Figure 5 we have that  $\xi_1(iz_2) = \xi_2(iz_2)$  and  $\xi_3(iz_3) = \xi_4(iz_3)$ . This is always the case if  $t_{c,1} < t < a/(a+b)$ . Then we have that  $\xi_1$  is analytic with a cut on  $[0, z_1] \cup [-iz_2, iz_2]$ ,  $\xi_2$  has a cut on  $[-z_1, 0] \cup [-iz_2, iz_2]$ ,  $\xi_3$  has a cut on  $[0, z_1] \cup [-iz_3, iz_3]$ , and  $\xi_4$  has a cut on  $[-z_1, 0] \cup [-iz_3, iz_3]$ . The sheet structure is then as shown in Figure 7.

For  $t = a/(a+b)$  we have that  $z_2 = z_3$  and for  $a/(a+b) < t < t_{c,2}$

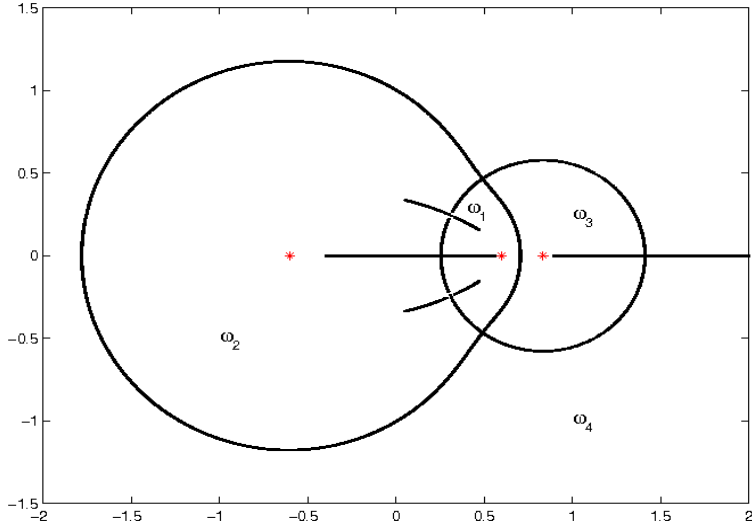


Figure 5: The image of the cross  $C = [-z_1, z_1] \cup [-iz_3, iz_3]$  in the  $v$ -plane for  $t_{c,1} < t < t_{c,2}$ . The values  $v = -a$ ,  $v = a$ , and  $v = \frac{1}{2b}$  are indicated with \*. These  $v$ -values correspond to  $\infty$  on the second, first and third sheets, respectively. The precise values used for the figure are  $a = b = 0.6$  and  $t = 0.45$ .

we find that the role of  $z_2$  and  $z_3$  are reversed, so that then the first and second sheets are connected along  $[-iz_3, iz_3]$  and the third and fourth along  $[-iz_2, iz_2]$ .

For  $t_{c,2} < t < 1$ , we have a similar sheet structure as in Figure 6, except that the cut on the vertical segment  $[-iz_3, iz_3]$  now connects the first and the second sheets.

### 3.5 Properties of $\xi_j$

The sheet structure induces jump relations between the  $\xi$ -functions along the cuts that we will use later on. At the branch point  $z_1$  we have for a real constant  $c_1 > 0$  that

$$\xi_1(z) = \xi_1(z_1) + c_1(z - z_1)^{1/2} + O(z - z_1), \quad (3.23)$$

$$\xi_3(z) = \xi_1(z_1) - c_1(z - z_1)^{1/2} + O(z - z_1). \quad (3.24)$$

In case  $t \in (0, t_{c,1}) \cup (t_{c,2}, 1)$  we also have that at the branch point  $z_2$  there is a real constant  $c_2 > 0$  such that

$$\xi_1(z) = \xi_1(z_2) - c_2(z_2 - z)^{1/2} + O(z_2 - z), \quad (3.25)$$

$$\xi_3(z) = \xi_1(z_2) + c_2(z_2 - z)^{1/2} + O(z_2 - z). \quad (3.26)$$



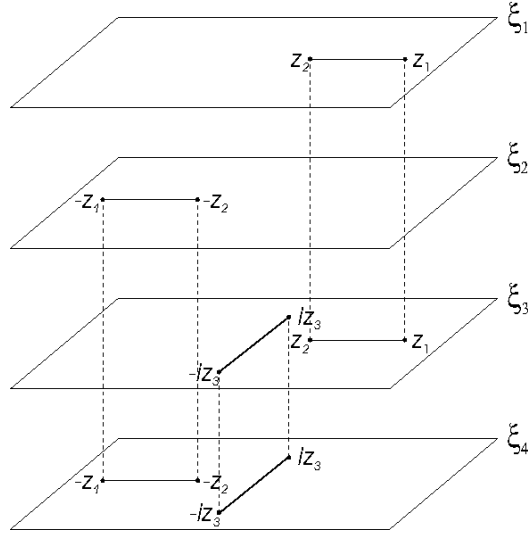


Figure 6: The sheet structure of the Riemann surface for  $ab < 1/2$  and  $0 < t < t_{c,1}$ .

Here the square root is taken with a branch cut along the negative real axis. Similar behavior also holds for the functions  $\xi_2$  and  $\xi_4$  near the branch points  $-z_1$  and  $-z_2$ .

From the sheet structure we also see how the  $\xi$ -functions are continued along the cuts. We will not list those relations explicitly, but they will be (tacitly) used in the future.

What is also important is that for any closed contour  $\gamma$  that does not intersect the cut on the  $j$ th sheet, we have

$$\frac{1}{2\pi i} \oint_{\gamma} \xi_j(s) ds \in \frac{1}{2}\mathbb{Z}. \quad (3.27)$$

This follows from the fact that the residues at infinity for each of the  $\xi_j$  functions is  $\pm\frac{1}{2}$ , see (3.18)–(3.21).

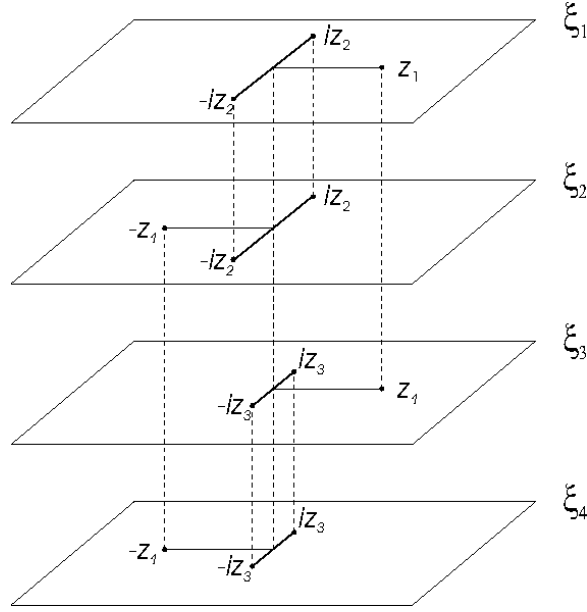


Figure 7: The sheet structure of the Riemann surface for  $ab < 1/2$  and  $t \in (t_{c,1}, t_{c,2})$ .

### 3.6 The $\lambda_j$ functions

The  $\lambda$ -functions are primitive functions of the  $\xi$ -functions. We define them as

$$\begin{aligned}
 \lambda_1(z) &= \int_{z_1}^z \xi_1(s) ds, \\
 \lambda_2(z) &= \int_{-z_{1+}}^z \xi_2(s) ds + c, \\
 \lambda_3(z) &= \int_{z_1}^z \xi_3(s) ds, \\
 \lambda_4(z) &= \int_{-z_{1-}}^z \xi_4(s) ds + c,
 \end{aligned} \tag{3.28}$$

where  $c$  is chosen so that  $\lambda_3(iz_3) = \lambda_4(iz_3)$  (if  $0 < t < a/(a+b)$ ), or  $\lambda_1(iz_3) = \lambda_2(iz_3)$  (if  $a/(a+b) < t < 1$ ). The path of integration in each integral in (3.28) is in  $\mathbb{C} \setminus (C \cup (-\infty, -z_1])$ .

From these definitions, and from the fact (3.27) that the periods of the  $\xi$ -functions are half integers, it then follows that  $e^{n\lambda}$  is analytic on the Riemann surface (recall  $n$  is even). That is, if  $C_{jk}$  is the cut connecting the  $j$ th and  $k$ th sheets, then

$$e^{n\lambda_{j\pm}} = e^{n\lambda_{k\mp}} \quad \text{on } C_{jk}. \tag{3.29}$$

The behavior as  $z \rightarrow \infty$  follows from (3.28) and (3.18)–(3.21) and is given by

$$\lambda_1(z) = \frac{z^2}{2t(1-t)} - \frac{az}{t} - \frac{1}{2} \ln z + l_1 + O\left(\frac{1}{z}\right), \quad (3.30)$$

$$\lambda_2(z) = \frac{z^2}{2t(1-t)} + \frac{az}{t} - \frac{1}{2} \ln z + l_2 + O\left(\frac{1}{z}\right), \quad (3.31)$$

$$\lambda_3(z) = \frac{bz}{1-t} + \frac{1}{2} \ln z + l_3 + O\left(\frac{1}{z}\right), \quad (3.32)$$

$$\lambda_4(z) = -\frac{bz}{1-t} + \frac{1}{2} \ln z + l_4 + O\left(\frac{1}{z}\right), \quad (3.33)$$

where  $l_1, l_2, l_3, l_4$  are certain integration constants.

## 4 Steepest descent analysis for case $0 < t < t_{c,1}$

We will do the steepest descent analysis in some detail for the case  $0 < t < t_{c,1}$ . The case  $t_{c,2} < t < 1$  follows from this by symmetry of the problem. For the case  $t_{c,1} < t < t_{c,2}$ , we refer to Section 6.

The steepest descent analysis is based on the one given in [4]. A major role is played by the Riemann surface, which for  $0 < t < t_{c,1}$ , has the sheet structure as shown in Figure 6.

### 4.1 First transformation: $Y \mapsto U$

In the first transformation we normalize the RH problem at infinity. We define

$$U(z) = L^n Y(z) \operatorname{diag} \left( e^{n(\lambda_1(z) - \frac{z^2}{2t(1-t)} + \frac{az}{t})}, e^{n(\lambda_2(z) - \frac{z^2}{2t(1-t)} - \frac{az}{t})}, \right. \\ \left. e^{n(\lambda_3(z) - \frac{bz}{1-t})}, e^{n(\lambda_4(z) + \frac{bz}{1-t})} \right), \quad (4.1)$$

where  $L$  is the constant diagonal matrix

$$L = \operatorname{diag} \left( e^{-l_1}, e^{-l_2}, e^{-l_3}, e^{-l_4} \right). \quad (4.2)$$

Here the constants  $l_j$ ,  $j = 1, 2, 3, 4$ , are the constants that appear in (3.30)–(3.33). Now  $U$  is defined and analytic in  $\mathbb{C} \setminus (\mathbb{R} \cup [-iz_3, iz_3])$ . Then (2.14), (3.30)–(3.33), and (4.1) imply that  $U$  is normalized at infinity:

$$U(z) = I + O(1/z) \quad \text{as } n \rightarrow \infty. \quad (4.3)$$

Using (4.1) and (2.13) we find the jumps for  $U$ . On the real line, we get

$$U_+ = U_- \begin{pmatrix} e^{n(\lambda_{1+}-\lambda_{1-})} & 0 & e^{n(\lambda_{3+}-\lambda_{1-})} & e^{n(\lambda_{4+}-\lambda_{1-})} \\ 0 & e^{n(\lambda_{2+}-\lambda_{2-})} & e^{n(\lambda_{3+}-\lambda_{2-})} & e^{n(\lambda_{4+}-\lambda_{2-})} \\ 0 & 0 & e^{n(\lambda_{3+}-\lambda_{3-})} & 0 \\ 0 & 0 & 0 & e^{n(\lambda_{4+}-\lambda_{4-})} \end{pmatrix}, \quad (4.4)$$

while on the vertical segment  $[-iz_3, iz_3]$ , which is oriented upwards (so that  $U_+(z)$  ( $U_-(z)$ ) is the limiting value of  $U(z')$  as  $z' \rightarrow z$  from the left (right) half-plane) we have the jump

$$U_+ = U_- \text{diag} \left( 1, 1, e^{n(\lambda_{3+}-\lambda_{3-})}, e^{n(\lambda_{4+}-\lambda_{4-})} \right). \quad (4.5)$$

Because of (3.29) we can simplify the jump (4.4) on the various parts of the real line. The result is the following RH problem for  $U$ :

### RH problem for $U$

- (1)  $U$  is analytic on  $\mathbb{C} \setminus (\mathbb{R} \cup [-iz_3, iz_3])$ .
- (2)  $U$  satisfies the following jumps on the real line:

$$U_+ = U_- \begin{pmatrix} 1 & 0 & e^{n(\lambda_{3+}-\lambda_{1-})} & e^{n(\lambda_{4+}-\lambda_{1-})} \\ 0 & 1 & e^{n(\lambda_{3+}-\lambda_{2-})} & e^{n(\lambda_{4+}-\lambda_{2-})} \\ 0 & 0 & 1 & 0 \\ 0 & 0 & 0 & 1 \end{pmatrix} \quad \text{on } (-\infty, -z_1), \quad (4.6)$$

$$U_+ = U_- \begin{pmatrix} 1 & 0 & e^{n(\lambda_{3+}-\lambda_{1-})} & e^{n(\lambda_{4+}-\lambda_{1-})} \\ 0 & e^{n(\lambda_{2+}-\lambda_{2-})} & e^{n(\lambda_{3+}-\lambda_{2-})} & 1 \\ 0 & 0 & 1 & 0 \\ 0 & 0 & 0 & e^{n(\lambda_{4+}-\lambda_{4-})} \end{pmatrix} \quad \text{on } (-z_1, -z_2), \quad (4.7)$$

$$U_+ = U_- \begin{pmatrix} 1 & 0 & e^{n(\lambda_{3+}-\lambda_{1-})} & e^{n(\lambda_{4+}-\lambda_{1-})} \\ 0 & 1 & e^{n(\lambda_{3+}-\lambda_{2-})} & e^{n(\lambda_{4+}-\lambda_{2-})} \\ 0 & 0 & 1 & 0 \\ 0 & 0 & 0 & 1 \end{pmatrix} \quad \text{on } (-z_2, 0) \cup (0, z_2), \quad (4.8)$$

$$U_+ = U_- \begin{pmatrix} e^{n(\lambda_{1+}-\lambda_{1-})} & 0 & 1 & e^{n(\lambda_{4+}-\lambda_{1-})} \\ 0 & 1 & e^{n(\lambda_{3+}-\lambda_{2-})} & e^{n(\lambda_{4+}-\lambda_{2-})} \\ 0 & 0 & e^{n(\lambda_{3+}-\lambda_{3-})} & 0 \\ 0 & 0 & 0 & 1 \end{pmatrix} \quad \text{on } (z_2, z_1), \quad (4.9)$$

$$U_+ = U_- \begin{pmatrix} 1 & 0 & e^{n(\lambda_3 - \lambda_1)} & e^{n(\lambda_4 - \lambda_1)} \\ 0 & 1 & e^{n(\lambda_3 - \lambda_2)} & e^{n(\lambda_4 - \lambda_2)} \\ 0 & 0 & 1 & 0 \\ 0 & 0 & 0 & 1 \end{pmatrix} \quad \text{on } (z_1, +\infty). \quad (4.10)$$

Finally, on the vertical segment, which is oriented upwards,

$$U_+ = U_- \text{diag} \left( 1, 1, e^{n(\lambda_{3+} - \lambda_{3-})}, e^{n(\lambda_{4+} - \lambda_{4-})} \right) \quad \text{on } (-iz_3, iz_3). \quad (4.11)$$

(3)  $U(z) = I + O(1/z)$  as  $z \rightarrow \infty$ .

Now it turns out that not all entries in the jump matrices for  $U$  are well-behaved as  $n \rightarrow \infty$ . Ideally, one would like to have exponentially decaying off-diagonal terms  $e^{n(\lambda_{j+} - \lambda_{k-})}$  in all of the jump matrices in (4.6)–(4.11), and oscillating diagonal entries  $e^{n(\lambda_{j+} - \lambda_{j-})}$ . However, this is not the case in the present situation. For example, the entry  $e^{n(\lambda_{3+} - \lambda_{3-})}$  in the jump matrix in (4.11) is exponentially increasing as  $n \rightarrow \infty$ , since  $\text{Re } \lambda_{3+} > \text{Re } \lambda_{3-}$  on the vertical segment  $(-iz_3, iz_3)$ .

## 4.2 Second transformation: $U \mapsto T$

We use a trick to remove the exponentially increasing entries. This involves the global opening of a lens, which was introduced in [4], and also used in [26].

We take a closed curve  $\Sigma$ , consisting of a part in the right half-plane that connects  $-iz_3$  and  $iz_3$ , that is symmetric with respect to the real axis, and that satisfies

$$\text{Re } \lambda_4(z) < \text{Re } \lambda_3(z) \quad \text{for } z \in \Sigma \cap \{\text{Re } z > 0\}. \quad (4.12)$$

The curve  $\Sigma$  intersects the positive real line in a point  $x^*$  and we assume that  $x^*$  is sufficiently large so that

$$\text{Re } \lambda_4(x) < \text{Re } \lambda_3(x) < \text{Re } \lambda_1(x) < \text{Re } \lambda_2(x) \quad \text{for } x \geq x^*, x \in \mathbb{R}.$$

The part of  $\Sigma$  in the left half-plane is the mirror image with respect to the imaginary axis. Then

$$\text{Re } \lambda_3(z) < \text{Re } \lambda_4(z) \quad \text{for } z \in \Sigma \cap \{\text{Re } z < 0\}, \quad (4.13)$$

and

$$\text{Re } \lambda_3(x) < \text{Re } \lambda_4(x) < \text{Re } \lambda_2(x) < \text{Re } \lambda_1(x) \quad \text{for } x \leq -x^*, x \in \mathbb{R}.$$

Note that the behavior (4.12)–(4.13) is valid near infinity because of (3.32)–(3.33) and we have that the inequalities remain valid in a domain whose boundary contains the branch points  $\pm iz_3$ .

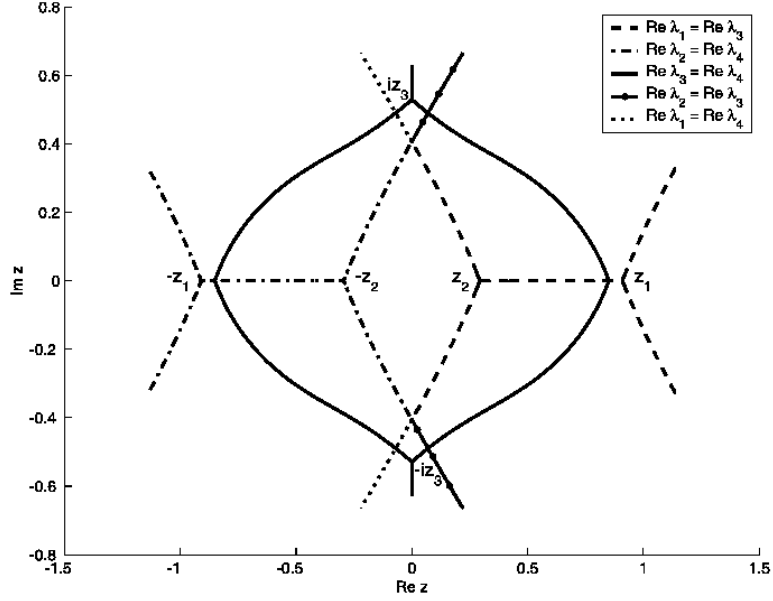


Figure 8: The behavior of the real part of  $\lambda_j - \lambda_k$  when  $a = b = 0.6$  and  $t = 0.05$ . Only some relevant curves are shown where two real parts coincide.

This is illustrated in Figures 8 and 9 where the solid curves are the curves where  $\text{Re } \lambda_3 = \text{Re } \lambda_4$ . We have three such curves that emanate at equal angles from  $iz_3$ . One of them extends to infinity along the positive imaginary axis. The other two continue to the branch point  $-iz_3$  and together form a closed contour. This closed contour can either contain the intervals  $[-z_1, -z_2]$  and  $[z_2, z_1]$  in its interior as in Figure 9, or it intersects these two intervals as in Figure 8.

For later convenience, we also choose  $\Sigma$  as the analytic continuation of the closed contour where  $\text{Re } \lambda_3 = \text{Re } \lambda_4$  in a neighborhood of  $\pm iz_3$ . For an example how to choose  $\Sigma$ , see Figure 10.

Now we are ready to introduce the second transformation, see also [4, section 4]. We define  $T$  as

$$T = U \quad \text{outside } \Sigma, \quad (4.14)$$

$$T = U \begin{pmatrix} 1 & 0 & 0 & 0 \\ 0 & 1 & 0 & 0 \\ 0 & 0 & 1 & 0 \\ 0 & 0 & -e^{n(\lambda_3 - \lambda_4)} & 1 \end{pmatrix} \quad \text{inside } \Sigma \text{ in the left half-plane,} \quad (4.15)$$

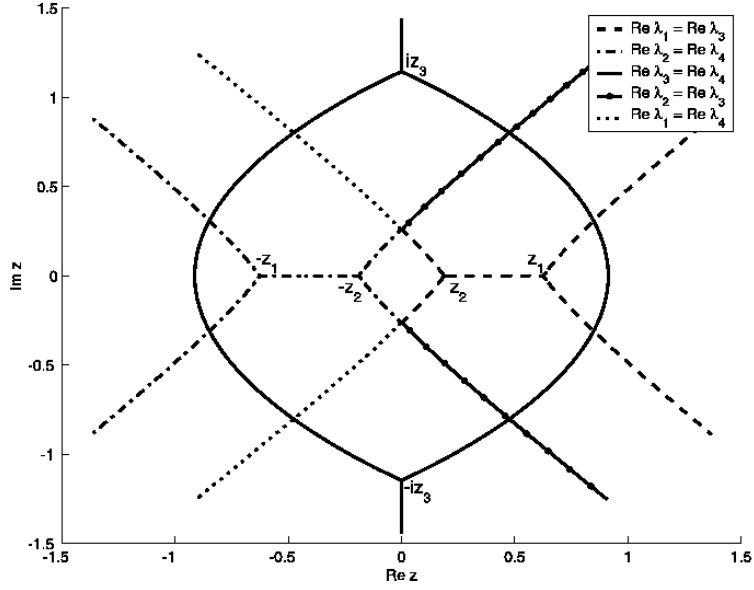


Figure 9: The behavior of the real part of  $\lambda_j - \lambda_k$  when  $a = b = 0.4$  and  $t = 0.025$ .

$$T = U \begin{pmatrix} 1 & 0 & 0 & 0 \\ 0 & 1 & 0 & 0 \\ 0 & 0 & 1 & -e^{n(\lambda_4 - \lambda_3)} \\ 0 & 0 & 0 & 1 \end{pmatrix} \quad \text{inside } \Sigma \text{ in the right half-plane.} \quad (4.16)$$

Then  $T$  has jumps on the contours shown in Figure 11 and a straightforward calculation shows that  $T$  satisfies the following RH problem:

### RH problem for $T$

(1)  $T$  is analytic on  $\mathbb{C} \setminus (\mathbb{R} \cup [-iz_3, iz_3] \cup \Sigma)$ .

(2) On the real line,  $T$  has the following jumps:

$$T_+ = T_- \begin{pmatrix} 1 & 0 & e^{n(\lambda_3 + -\lambda_{1-})} & e^{n(\lambda_4 + -\lambda_{1-})} \\ 0 & 1 & e^{n(\lambda_3 + -\lambda_{2-})} & e^{n(\lambda_4 + -\lambda_{2-})} \\ 0 & 0 & 1 & 0 \\ 0 & 0 & 0 & 1 \end{pmatrix} \quad \text{on } (-\infty, -x^*), \quad (4.17)$$

$$T_+ = T_- \begin{pmatrix} 1 & 0 & 0 & e^{n(\lambda_4 + -\lambda_{1-})} \\ 0 & 1 & 0 & e^{n(\lambda_4 + -\lambda_{2-})} \\ 0 & 0 & 1 & 0 \\ 0 & 0 & 0 & 1 \end{pmatrix} \quad \text{on } (-x^*, -z_1), \quad (4.18)$$

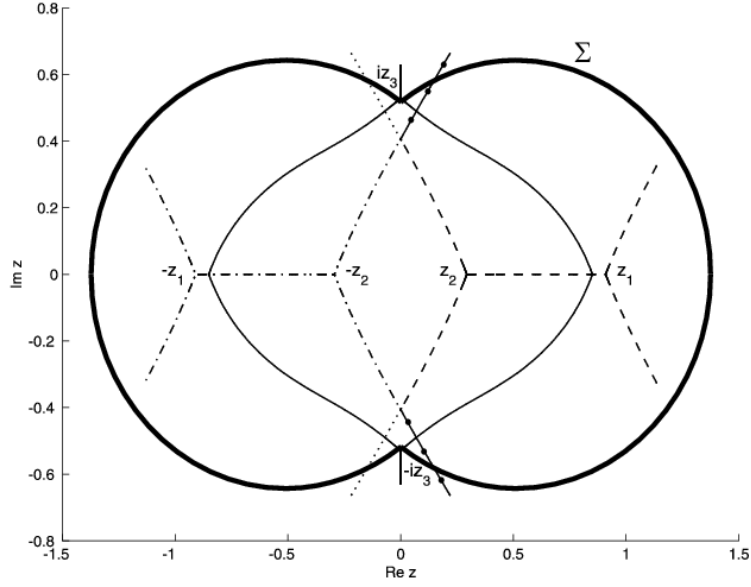


Figure 10: Opening of the global lens  $\Sigma$  that connects  $\pm iz_3$ . It is such that  $\text{Re } \lambda_3 > \text{Re } \lambda_4$  on  $\Sigma$  in the right half-plane, and  $\text{Re } \lambda_4 > \text{Re } \lambda_3$  on  $\Sigma$  in the left half-plane. Here we have taken  $a = b = 0.6$  and  $t = 0.05$ .

$$T_+ = T_- \begin{pmatrix} 1 & 0 & 0 & e^{n(\lambda_{4+} - \lambda_{1-})} \\ 0 & e^{n(\lambda_{2+} - \lambda_{2-})} & 0 & 1 \\ 0 & 0 & 1 & 0 \\ 0 & 0 & 0 & e^{n(\lambda_{4+} - \lambda_{4-})} \end{pmatrix} \quad \text{on } (-z_1, -z_2), \quad (4.19)$$

$$T_+ = T_- \begin{pmatrix} 1 & 0 & 0 & e^{n(\lambda_{4+} - \lambda_{1-})} \\ 0 & 1 & 0 & e^{n(\lambda_{4+} - \lambda_2)} \\ 0 & 0 & 1 & 0 \\ 0 & 0 & 0 & 1 \end{pmatrix} \quad \text{on } (-z_2, 0), \quad (4.20)$$

$$T_+ = T_- \begin{pmatrix} 1 & 0 & e^{n(\lambda_{3+} - \lambda_{1-})} & 0 \\ 0 & 1 & e^{n(\lambda_{3+} - \lambda_2)} & 0 \\ 0 & 0 & 1 & 0 \\ 0 & 0 & 0 & 1 \end{pmatrix} \quad \text{on } (0, z_2), \quad (4.21)$$

$$T_+ = T_- \begin{pmatrix} e^{n(\lambda_{1+} - \lambda_{1-})} & 0 & 1 & 0 \\ 0 & 1 & e^{n(\lambda_{3+} - \lambda_2)} & 0 \\ 0 & 0 & e^{n(\lambda_{3+} - \lambda_{3-})} & 0 \\ 0 & 0 & 0 & 1 \end{pmatrix} \quad \text{on } (z_2, z_1), \quad (4.22)$$



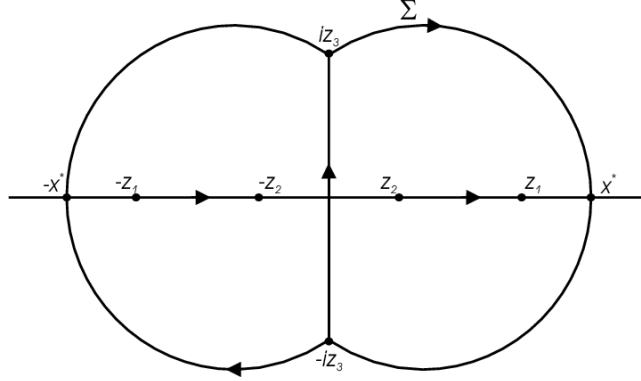


Figure 11: Jump contour for the RH problem for  $T$ . The contour  $\Sigma$  has clockwise orientation. The  $4 \times 4$  matrix valued function  $T$  is analytic outside these contours, and has jumps (4.17)–(4.27) along the various parts of the contour.

$$T_+ = T_- \begin{pmatrix} 1 & 0 & e^{n(\lambda_3 - \lambda_1)} & 0 \\ 0 & 1 & e^{n(\lambda_3 - \lambda_2)} & 0 \\ 0 & 0 & 1 & 0 \\ 0 & 0 & 0 & 1 \end{pmatrix} \quad \text{on } (z_1, x^*), \quad (4.23)$$

$$T_+ = T_- \begin{pmatrix} 1 & 0 & e^{n(\lambda_3 - \lambda_1)} & e^{n(\lambda_4 - \lambda_1)} \\ 0 & 1 & e^{n(\lambda_3 - \lambda_2)} & e^{n(\lambda_4 - \lambda_2)} \\ 0 & 0 & 1 & 0 \\ 0 & 0 & 0 & 1 \end{pmatrix} \quad \text{on } (x^*, +\infty). \quad (4.24)$$

On the vertical segment (with upwards orientation), we have

$$T_+ = T_- \begin{pmatrix} 1 & 0 & 0 & 0 \\ 0 & 1 & 0 & 0 \\ 0 & 0 & 0 & 1 \\ 0 & 0 & -1 & e^{n(\lambda_{4+} - \lambda_{4-})} \end{pmatrix} \quad \text{on } (-iz_3, iz_3). \quad (4.25)$$

The jumps on  $\Sigma$  are as follows, where we take clockwise orientation on  $\Sigma$ , so that  $T_+(z)$  ( $T_-(z)$ ) for  $z \in \Sigma$ , is the limiting value of  $T(z')$  as  $z' \rightarrow z$  from outside (inside) of  $\Sigma$ :

$$T_+ = T_- \begin{pmatrix} 1 & 0 & 0 & 0 \\ 0 & 1 & 0 & 0 \\ 0 & 0 & 1 & 0 \\ 0 & 0 & e^{n(\lambda_3 - \lambda_4)} & 1 \end{pmatrix} \quad \text{on } \{z \in \Sigma \mid \operatorname{Re} z < 0\}, \quad (4.26)$$

$$T_+ = T_- \begin{pmatrix} 1 & 0 & 0 & 0 \\ 0 & 1 & 0 & 0 \\ 0 & 0 & 1 & e^{n(\lambda_4 - \lambda_3)} \\ 0 & 0 & 0 & 1 \end{pmatrix} \quad \text{on } \{z \in \Sigma \mid \operatorname{Re} z > 0\} \quad (4.27)$$

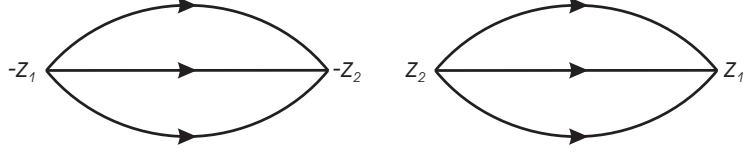


Figure 12: Opening of the lenses  $\Gamma_1$  and  $\Gamma_2$  around the intervals  $[-z_1, -z_2]$  and  $[z_2, z_1]$ .

(3)  $T(z) = I + O(1/z)$  as  $z \rightarrow \infty$ .

Now it follows that the jump matrix in (4.25) on the vertical segment  $(-iz_3, iz_3)$  tends to a constant matrix since  $\operatorname{Re} \lambda_{4+} < \operatorname{Re} \lambda_{4-}$ . This may also be deduced from Figures 8 and 9, since we have  $\operatorname{Re} \lambda_3 < \operatorname{Re} \lambda_4$  in the right half-plane within the closed contour in these figures. The strict inequality remains valid up to the vertical segment  $(-iz_3, iz_3)$  so that  $\operatorname{Re} \lambda_{3-} < \operatorname{Re} \lambda_{4-}$ , since the orientation of the segment is upwards. Since  $\operatorname{Re} \lambda_{4\pm} = \operatorname{Re} \lambda_{3\mp}$  the inequality  $\operatorname{Re} \lambda_{4+} < \operatorname{Re} \lambda_{4-}$  follows.

All the jump matrices on the real line tend to the identity matrix as  $n \rightarrow \infty$ , except for the ones on the intervals  $(-z_1, -z_2)$  and  $(z_2, z_1)$ . The 1,1-entry and the 3,3-entry of the jump matrix on  $(z_2, z_1)$ , see (4.22), are rapidly oscillating for large  $n$ , and the same holds for the 2,2-entry and the 4,4-entry of the jump matrix on  $(-z_1, -z_2)$ , see (4.19). These oscillating entries are turned into exponentially decaying ones in a standard way by opening lenses around the intervals  $[-z_1, -z_2]$  and  $[z_2, z_1]$ . This will be done next.

### 4.3 Third transformation: $T \mapsto S$

We now turn the oscillatory entries on the diagonal of (4.19) and (4.22) into exponentially decaying ones. This is done in a standard way by opening lenses  $\Gamma_1$  and  $\Gamma_2$  in (small) neighborhoods of  $(-z_1, -z_2)$  and  $(z_2, z_1)$ , respectively, as shown in Figure 12. Define  $S$  as follows:

$$S = T \quad \text{outside } \Gamma_1 \text{ and } \Gamma_2, \quad (4.28)$$

$$S = T \begin{pmatrix} 1 & 0 & 0 & 0 \\ 0 & 1 & 0 & 0 \\ 0 & 0 & 1 & 0 \\ 0 & -e^{n(\lambda_2 - \lambda_4)} & 0 & 1 \end{pmatrix} \quad \text{in the upper lens region around } [-z_1, -z_2], \quad (4.29)$$

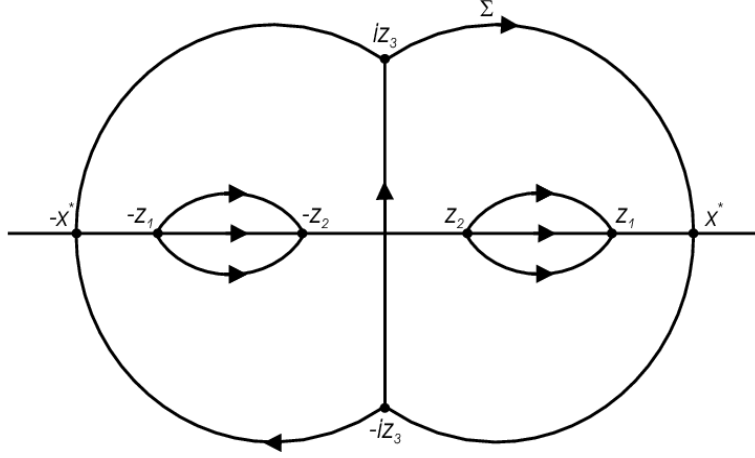


Figure 13: Jump contour for the RH problem for  $S$ . The contour  $\Sigma$  has clockwise orientation and the upper and lower lips of the lenses are oriented from left to right. The  $4 \times 4$  matrix valued function  $S$  is analytic outside these contours, and has jumps (4.33)–(4.45) along the various parts of the contour.

$$S = T \begin{pmatrix} 1 & 0 & 0 & 0 \\ 0 & 1 & 0 & 0 \\ 0 & 0 & 1 & 0 \\ 0 & e^{n(\lambda_2 - \lambda_4)} & 0 & 1 \end{pmatrix} \quad \text{in the lower lens region around } [-z_1, -z_2], \quad (4.30)$$

$$S = T \begin{pmatrix} 1 & 0 & 0 & 0 \\ 0 & 1 & 0 & 0 \\ -e^{n(\lambda_1 - \lambda_3)} & 0 & 1 & 0 \\ 0 & 0 & 0 & 1 \end{pmatrix} \quad \text{in the upper lens region around } [z_2, z_1], \quad (4.31)$$

$$S = T \begin{pmatrix} 1 & 0 & 0 & 0 \\ 0 & 1 & 0 & 0 \\ e^{n(\lambda_1 - \lambda_3)} & 0 & 1 & 0 \\ 0 & 0 & 0 & 1 \end{pmatrix} \quad \text{in the lower lens region around } [z_2, z_1]. \quad (4.32)$$

Then  $S$  satisfies the following RH problem on the contour shown in Figure 13:

**RH problem for  $S$**

- (1)  $S$  is analytic on  $\mathbb{C} \setminus (\mathbb{R} \cup \Sigma \cup \Gamma_1 \cup \Gamma_2 \cup [-iz_3, iz_3])$ ,

(2) On the real line,  $S$  has the following jumps:

$$S_+ = S_- \begin{pmatrix} 1 & 0 & e^{n(\lambda_{3+}-\lambda_{1-})} & e^{n(\lambda_{4+}-\lambda_{1-})} \\ 0 & 1 & e^{n(\lambda_{3+}-\lambda_{2-})} & e^{n(\lambda_{4+}-\lambda_{2-})} \\ 0 & 0 & 1 & 0 \\ 0 & 0 & 0 & 1 \end{pmatrix} \text{ on } (-\infty, -x^*), \quad (4.33)$$

$$S_+ = S_- \begin{pmatrix} 1 & 0 & 0 & e^{n(\lambda_{4+}-\lambda_{1-})} \\ 0 & 1 & 0 & e^{n(\lambda_{4+}-\lambda_{2-})} \\ 0 & 0 & 1 & 0 \\ 0 & 0 & 0 & 1 \end{pmatrix} \text{ on } (-x^*, -z_1), \quad (4.34)$$

$$S_+ = S_- \begin{pmatrix} 1 & -e^{n(\lambda_{2+}-\lambda_{1-})} & 0 & e^{n(\lambda_{4+}-\lambda_{1-})} \\ 0 & 0 & 0 & 1 \\ 0 & 0 & 1 & 0 \\ 0 & -1 & 0 & 0 \end{pmatrix} \text{ on } (-z_1, -z_2), \quad (4.35)$$

$$S_+ = S_- \begin{pmatrix} 1 & 0 & 0 & e^{n(\lambda_{4+}-\lambda_{1-})} \\ 0 & 1 & 0 & e^{n(\lambda_{4+}-\lambda_{2-})} \\ 0 & 0 & 1 & 0 \\ 0 & 0 & 0 & 1 \end{pmatrix} \text{ on } (-z_2, 0), \quad (4.36)$$

$$S_+ = S_- \begin{pmatrix} 1 & 0 & e^{n(\lambda_{3+}-\lambda_{1-})} & 0 \\ 0 & 1 & e^{n(\lambda_{3+}-\lambda_{2-})} & 0 \\ 0 & 0 & 1 & 0 \\ 0 & 0 & 0 & 1 \end{pmatrix} \text{ on } (0, z_2), \quad (4.37)$$

$$S_+ = S_- \begin{pmatrix} 0 & 0 & 1 & 0 \\ -e^{n(\lambda_{1+}-\lambda_2)} & 1 & e^{n(\lambda_{3+}-\lambda_2)} & 0 \\ -1 & 0 & 0 & 0 \\ 0 & 0 & 0 & 1 \end{pmatrix} \text{ on } (z_2, z_1), \quad (4.38)$$

$$S_+ = S_- \begin{pmatrix} 1 & 0 & e^{n(\lambda_3-\lambda_1)} & 0 \\ 0 & 1 & e^{n(\lambda_3-\lambda_2)} & 0 \\ 0 & 0 & 1 & 0 \\ 0 & 0 & 0 & 1 \end{pmatrix} \text{ on } (z_1, x^*), \quad (4.39)$$

$$S_+ = S_- \begin{pmatrix} 1 & 0 & e^{n(\lambda_3-\lambda_1)} & e^{n(\lambda_4-\lambda_1)} \\ 0 & 1 & e^{n(\lambda_3-\lambda_2)} & e^{n(\lambda_4-\lambda_2)} \\ 0 & 0 & 1 & 0 \\ 0 & 0 & 0 & 1 \end{pmatrix} \text{ on } (x^*, +\infty). \quad (4.40)$$

On the vertical segment, we have that

$$S_+ = S_- \begin{pmatrix} 1 & 0 & 0 & 0 \\ 0 & 1 & 0 & 0 \\ 0 & 0 & 0 & 1 \\ 0 & 0 & -1 & e^{n(\lambda_{4+} - \lambda_{4-})} \end{pmatrix} \quad \text{on } (-iz_3, iz_3). \quad (4.41)$$

On  $\Sigma$ , the jumps of  $S$  are

$$S_+ = S_- \begin{pmatrix} 1 & 0 & 0 & 0 \\ 0 & 1 & 0 & 0 \\ 0 & 0 & 1 & 0 \\ 0 & 0 & e^{n(\lambda_3 - \lambda_4)} & 1 \end{pmatrix} \quad \text{on } \Sigma \text{ in the left half-plane,} \quad (4.42)$$

$$S_+ = S_- \begin{pmatrix} 1 & 0 & 0 & 0 \\ 0 & 1 & 0 & 0 \\ 0 & 0 & 1 & e^{n(\lambda_4 - \lambda_3)} \\ 0 & 0 & 0 & 1 \end{pmatrix} \quad \text{on } \Sigma \text{ in the right half-plane.} \quad (4.43)$$

The jumps on the lenses  $\Gamma_1$  and  $\Gamma_2$  around  $[-z_1, -z_2]$  and  $[z_2, z_1]$  are

$$S_+ = S_- \begin{pmatrix} 1 & 0 & 0 & 0 \\ 0 & 1 & 0 & 0 \\ 0 & 0 & 1 & 0 \\ 0 & e^{n(\lambda_2 - \lambda_4)} & 0 & 1 \end{pmatrix} \quad \text{on } \Gamma_1, \quad (4.44)$$

$$S_+ = S_- \begin{pmatrix} 1 & 0 & 0 & 0 \\ 0 & 1 & 0 & 0 \\ e^{n(\lambda_1 - \lambda_3)} & 0 & 1 & 0 \\ 0 & 0 & 0 & 1 \end{pmatrix} \quad \text{on } \Gamma_2. \quad (4.45)$$

(3)  $S = I + O(1/z)$  as  $z \rightarrow \infty$ .

Now it can be checked that all non-constant entries in the jump matrices for  $S$  tend to 0 as  $n \rightarrow \infty$ . This could be done by completing the Figures 8 and 9 by drawing all curves where  $\text{Re } \lambda_j = \text{Re } \lambda_k$  for  $j \neq k$  from which one can deduce the sign of  $\text{Re}(\lambda_j - \lambda_k)$  in various regions in the complex plane.

For the jumps on  $(-z_1, -z_2)$  and  $(z_2, z_1)$  one can also use a Cauchy-Riemann type argument. For the interval  $(z_2, z_1)$  this is based on the fact that  $(\lambda_1 - \lambda_3)_+$  is purely imaginary on  $(z_2, z_1)$  and its derivative is  $(\xi_1 - \xi_3)_+ = 2i \text{Im } \xi_{1+}$  where  $\text{Im } \xi_{1+} > 0$ . Then by the Cauchy-Riemann equations we have that  $\text{Re}(\lambda_1 - \lambda_3) < 0$  in a neighborhood above  $(z_2, z_1)$ .

#### 4.4 Parametrix away from the branch points

We are now going to solve the model RH problem, where we ignore all exponentially small entries in the jump matrices for  $S$ . So we only keep the jumps on  $(-z_1, -z_2)$ ,  $(z_2, z_1)$ , and  $(-iz_3, iz_3)$  (which are also the cuts for the Riemann surface) and we look for a  $4 \times 4$  matrix valued function  $N$  that satisfies the following RH problem:

##### RH problem for $N$

- (1)  $N$  is analytic on  $\mathbb{C} \setminus ([-z_1, -z_2] \cup [z_2, z_1] \cup [-iz_3, iz_3])$ ,
- (2)  $N$  satisfies the following jumps along the cuts:

$$N_+ = N_- \begin{pmatrix} 1 & 0 & 0 & 0 \\ 0 & 0 & 0 & 1 \\ 0 & 0 & 1 & 0 \\ 0 & -1 & 0 & 0 \end{pmatrix} \quad \text{on } (-z_1, -z_2), \quad (4.46)$$

$$N_+ = N_- \begin{pmatrix} 0 & 0 & 1 & 0 \\ 0 & 1 & 0 & 0 \\ -1 & 0 & 0 & 0 \\ 0 & 0 & 0 & 1 \end{pmatrix} \quad \text{on } (z_2, z_1), \quad (4.47)$$

$$N_+ = N_- \begin{pmatrix} 1 & 0 & 0 & 0 \\ 0 & 1 & 0 & 0 \\ 0 & 0 & 0 & 1 \\ 0 & 0 & -1 & 0 \end{pmatrix} \quad \text{on } (-iz_3, iz_3), \quad (4.48)$$

- (3) as  $z \rightarrow \infty$ , we have that

$$N(z) \rightarrow I + O(1/z). \quad (4.49)$$

By means of the rational parametrization of the Riemann surface we can transform this problem to the complex  $v$ -plane and thereby solve this RH problem explicitly.

Recall that we have the mapping  $v = v_k(z)$  that maps the  $k$ th sheet of the Riemann surface to the part  $\omega_k$  of the  $v$ -plane, see also Figure 4. We look for a solution for the RH problem for  $N$  in the form

$$N(z) = (F_j(v_k(z)))_{j,k=1,\dots,4}$$

where  $F_j$ ,  $j = 1, \dots, 4$  are four functions on the  $v$ -plane. Then the jump conditions on  $N$  are satisfied if the  $F_j$  are analytic except for the parts of the boundaries of the domains  $\omega_k$  that are indicated in Figure 14, and on these parts we have  $F_{j+} = -F_{j-}$ . The asymptotic condition on  $N$  is satisfied provided that

$$F_j(v_k(\infty)) = \delta_{jk}, \quad \text{for } j, k = 1, \dots, 4.$$

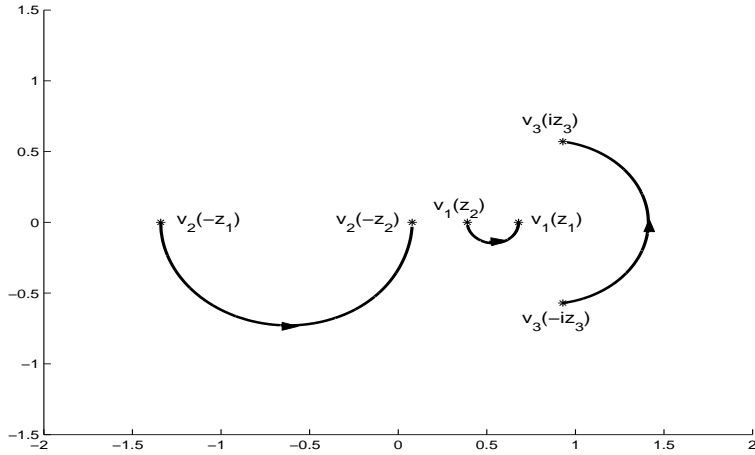


Figure 14: Jump contours in the  $v$ -plane for the scalar RH problems for the functions  $F_j$ ,  $j = 1, 2, 3, 4$ .

For each  $j$ , we then have a scalar RH problem for  $F_j$  that can be solved explicitly with elementary functions.

The precise form of  $F_j$  is not important for what follows, but we do need that  $F_j(v)$  behaves like  $(v - v_0)^{-1/2}$  as  $v \rightarrow v_0$  and  $v_0$  is one of the endpoints of the jump contour in Figure 14. For  $N$  this implies that

$$N(z) = O\left((z - z_0)^{-1/4}\right) \quad \text{as } z \rightarrow z_0,$$

where  $z_0$  is any of the branch points  $\pm z_1, \pm z_2, \pm iz_3$ .

#### 4.5 Parametrix near the branch points

The jump matrices on  $N$  and  $S$  are not uniformly close to each other near the branch points. That is why we need to treat these points separately, and construct a local parametrix  $P$  around these branch points.

We are going to construct a local parametrix around  $z_1$ . The local parametrices around  $-z_1, \pm z_2, \pm iz_3$  can be found in a similar way, and are therefore not further discussed here. Consider a small but fixed disc  $U_\delta$  with radius  $\delta$  around  $z_1$  that does not contain  $z_2$ . We then look for a  $4 \times 4$  matrix valued function  $P$  such that

##### **RH problem for $P$ around $z_1$**

- (1)  $P$  is analytic for  $z \in U_{\delta_0} \setminus (\Gamma_2 \cup \mathbb{R})$ , for some  $\delta_0 > \delta$ ,

(2)  $P$  has the following jumps on the real line:

$$P_+ = P_- \begin{pmatrix} 0 & 0 & 1 & 0 \\ 0 & 1 & 0 & 0 \\ -1 & 0 & 0 & 0 \\ 0 & 0 & 0 & 1 \end{pmatrix} \quad \text{on } U_\delta \cap [z_2, z_1], \quad (4.50)$$

$$P_+ = P_- \begin{pmatrix} 1 & 0 & e^{n(\lambda_3 - \lambda_1)} & 0 \\ 0 & 1 & 0 & 0 \\ 0 & 0 & 1 & 0 \\ 0 & 0 & 0 & 1 \end{pmatrix} \quad \text{on } U_\delta \cap [z_1, +\infty), \quad (4.51)$$

and on the lens  $\Gamma_2$  around  $[z_2, z_1]$ , we have

$$P_+ = P_- \begin{pmatrix} 1 & 0 & 0 & 0 \\ 0 & 1 & 0 & 0 \\ e^{n(\lambda_1 - \lambda_3)} & 0 & 1 & 0 \\ 0 & 0 & 0 & 1 \end{pmatrix} \quad \text{on } U_\delta \cap \Gamma_2. \quad (4.52)$$

(3) As  $n \rightarrow \infty$ ,

$$P(z) = N(z)(I + O(1/n)) \quad \text{uniformly for } z \in \partial U_\delta \setminus (\mathbb{R} \cup \Gamma_2). \quad (4.53)$$

Note that the jumps for  $P$  are not exactly the same as the jumps for  $S$ . They differ by the entries  $e^{n(\lambda_3 + -\lambda_2)}$  and  $e^{n(\lambda_1 + -\lambda_2)}$  which are exponentially small as  $n \rightarrow \infty$ .

The RH problem is solved in a standard way with Airy functions [15, 16, 4, 6]. We have that

$$f_1(z) = \left[ \frac{3}{4}(\lambda_1 - \lambda_3)(z) \right]^{2/3} \quad (4.54)$$

is a conformal map that maps a neighborhood of  $z_1$  onto a neighborhood of the origin such that  $f_1(z)$  is real and positive for  $z > z_1$ . We open the lens around  $[z_2, z_1]$  such that  $f_1$  maps the part of  $\Gamma_2$  in this neighborhood of  $z_1$  to the rays with angles  $\frac{2\pi}{3}$  and  $-\frac{2\pi}{3}$ , respectively. We put

$$y_0(s) = \text{Ai}(s), \quad y_1(s) = e^{2\pi i/3} \text{Ai}(e^{2\pi i/3} s), \quad y_2(s) = e^{-2\pi i/3} \text{Ai}(e^{-2\pi i/3} s), \quad (4.55)$$



where  $\text{Ai}$  is the usual Airy function. Define the matrix  $\Psi$  by

$$\Psi(s) = \begin{pmatrix} y_0(s) & 0 & -y_2(s) & 0 \\ 0 & 1 & 0 & 0 \\ y'_0(s) & 0 & -y'_2(s) & 0 \\ 0 & 0 & 0 & 1 \end{pmatrix} \quad \text{for } \arg s \in (0, 2\pi/3), \quad (4.56)$$

$$\Psi(s) = \begin{pmatrix} -y_1(s) & 0 & -y_2(s) & 0 \\ 0 & 1 & 0 & 0 \\ -y'_1(s) & 0 & -y'_2(s) & 0 \\ 0 & 0 & 0 & 1 \end{pmatrix} \quad \text{for } \arg s \in (2\pi/3, \pi), \quad (4.57)$$

$$\Psi(s) = \begin{pmatrix} -y_2(s) & 0 & y_1(s) & 0 \\ 0 & 1 & 0 & 0 \\ -y'_2(s) & 0 & y'_1(s) & 0 \\ 0 & 0 & 0 & 1 \end{pmatrix} \quad \text{for } \arg s \in (-\pi, -2\pi/3), \quad (4.58)$$

$$\Psi(s) = \begin{pmatrix} y_0(s) & 0 & y_1(s) & 0 \\ 0 & 1 & 0 & 0 \\ y'_0(s) & 0 & y'_1(s) & 0 \\ 0 & 0 & 0 & 1 \end{pmatrix} \quad \text{for } \arg s \in (-2\pi/3, 0). \quad (4.59)$$

Then, for any analytic prefactor  $E$ , we have that

$$P(z) = E(z)\Psi \left( n^{2/3} f_1(z) \right) \text{diag} \left( e^{\frac{\pi}{2}(\lambda_1(z) - \lambda_3(z))}, 1, e^{-\frac{\pi}{2}(\lambda_1(z) - \lambda_3(z))}, 1 \right) \quad (4.60)$$

satisfies the parts (1) and (2) of the RH problem for  $P$ . If we choose  $E$  as

$$E = \sqrt{\pi} N \begin{pmatrix} 1 & 0 & -1 & 0 \\ 0 & 1 & 0 & 0 \\ -i & 0 & -i & 0 \\ 0 & 0 & 0 & 1 \end{pmatrix} \begin{pmatrix} n^{1/6} f_1^{1/4} & 0 & 0 & 0 \\ 0 & 1 & 0 & 0 \\ 0 & 0 & n^{-1/6} f_1^{-1/4} & 0 \\ 0 & 0 & 0 & 1 \end{pmatrix} \quad (4.61)$$

then  $E$  is analytic and the part (3) is satisfied as well.

#### 4.6 Fourth transformation: $S \mapsto R$

In the final transformation, we define the matrix valued function  $R$  as

$$R(z) = S(z)P(z)^{-1} \quad \text{in (small) discs around } \pm z_1, \pm z_2 \text{ and } \pm iz_3, \quad (4.62)$$

$$R(z) = S(z)N(z)^{-1} \quad \text{outside the discs.} \quad (4.63)$$

Then  $R$  is defined and is analytic (more precisely, has analytic continuation to the region) outside the contour shown in Figure 15.

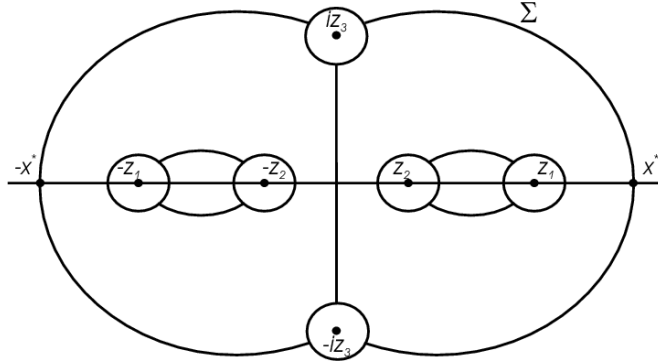


Figure 15: Jump contour for the RH problem for  $R$ . The  $4 \times 4$  matrix valued function  $R$  is analytic outside these contours, and has jumps  $R_+ = R_-(I + O(1/n))$  uniformly on all parts of the contour.

From the matching condition (4.53) (and similar ones around the other branch points), it follows that on the circles around the branch points there is a jump

$$R_+ = R_-(I + O(1/n)) \quad \text{uniformly as } n \rightarrow \infty. \quad (4.64)$$

On the remaining contours, the jump is given by

$$R_+ = R_-(I + O(e^{-cn})) \quad \text{as } n \rightarrow \infty \quad (4.65)$$

for some constant  $c > 0$ . Together with the asymptotic condition

$$R(z) = I + O(1/z) \quad \text{as } z \rightarrow \infty, \quad (4.66)$$

it then follows as in [4, 14, 15, 16, 22] that

$$R(z) = I + O\left(\frac{1}{n(|z|+1)}\right) \quad \text{as } n \rightarrow \infty, \quad (4.67)$$

uniformly for  $z \in \mathbb{C} \setminus \Gamma_R$ , where  $\Gamma_R$  is the jump contour for the RH problem for  $R$ , see Figure 15.

## 5 Proofs of theorems for case $0 < t < t_{c,1}$

Having (4.67) we can now prove Theorems 2.1–2.3 in the same way as in [6].

## 5.1 Proof of Theorem 2.1

Take  $x, y \in (z_2, z_1)$ . We follow the transformations  $Y \mapsto U \mapsto T \mapsto S$ , to obtain from (2.16) that

$$K_n(x, y) = \frac{e^{n(h(y)-h(x))}}{2\pi i(x-y)} \begin{pmatrix} -e^{in\operatorname{Im} \lambda_{1+}(y)} & 0 & e^{-in\operatorname{Im} \lambda_{1+}(y)} & e^{n(\lambda_4(y)-\operatorname{Re} \lambda_{1+}(y))} \end{pmatrix} \\ \times S_+^{-1}(y)S_+(x) \begin{pmatrix} e^{-in\operatorname{Im} \lambda_{1+}(x)} \\ 0 \\ e^{in\operatorname{Im} \lambda_{1+}(x)} \\ 0 \end{pmatrix}, \quad (5.1)$$

where

$$h(x) = \frac{1}{2} (\operatorname{Re} \lambda_{1+}(x) + \operatorname{Re} \lambda_{3+}(x)) - \frac{x^2}{2(1-t)} \text{ for } x > 0.$$

As in [6, Section 9] we obtain from (4.67) that

$$S_+^{-1}(y)S_+(x) = I + O(x-y) \quad \text{as } y \rightarrow x \quad (5.2)$$

uniformly in  $n$ , and therefore we get that

$$K_n(x, y) = e^{n(h(y)-h(x))} \left( \frac{\sin(n\operatorname{Im} (\lambda_{1+}(x) - \lambda_{1+}(y)))}{\pi(x-y)} + O(1) \right), \quad (5.3)$$

where the  $O(1)$  holds uniformly in  $n$ . Letting  $y \rightarrow x$  we find

$$K_n(x, x) = \frac{n}{\pi} \operatorname{Im} \xi_{1+}(x) + O(1). \quad (5.4)$$

For  $x \in (-z_2, -z_1)$  we get the similar relation but with  $\xi_{1+}(x)$  replaced by  $\xi_{2+}(x)$ . Thus (2.4) holds with  $\rho$  defined by

$$\rho(x) = \begin{cases} \frac{1}{\pi} \operatorname{Im} \xi_{1+}(x) & \text{for } x > 0, \\ \frac{1}{\pi} \operatorname{Im} \xi_{2+}(x) & \text{for } x < 0. \end{cases} \quad (5.5)$$

The further statements in Theorem 2.1 are now easy consequences of the properties of  $\xi_1$  and  $\xi_2$ .

## 5.2 Proof of Theorem 2.2

Let  $x_0 \in (z_2, z_1)$  and take

$$x = x_0 + \frac{u}{n\rho(x_0)}, \quad y = x_0 + \frac{v}{n\rho(x_0)}.$$

Then for  $n$  large enough, we have  $x, y \in (z_2, z_1)$ , so that (5.1) holds. Thus

$$\frac{1}{n\rho(x_0)} \hat{K}_n(x, y) = \frac{\sin(n(\operatorname{Im} \lambda_{1+}(x) - \operatorname{Im} \lambda_{1+}(y)))}{\pi(u-v)} + O\left(\frac{1}{n}\right).$$

This leads to (2.10) as in [6, section 9.2].

The proof for  $x_0 \in (-z_2, -z_1)$  is similar.

### 5.3 Proof of Theorem 2.3

Take  $x = z_1 + \frac{u}{(c_1 n)^{2/3}}$  and  $y = z_1 + \frac{v}{(c_1 n)^{2/3}}$ . If  $u, v < 0$ , then we can follow the transformations  $Y \mapsto U \mapsto T \mapsto S \mapsto R$ , to find from (2.16)

$$\begin{aligned} \frac{1}{(c_1 n)^{2/3}} \hat{K}_n(x, y) &= \frac{1}{2\pi i(u-v)} \begin{pmatrix} -1 & 0 & 1 & e^{n\operatorname{Re}(\lambda_{4+}(y) - \lambda_{1+}(y))} \end{pmatrix} \\ &\quad \times \Psi_+^{-1} \left( n^{2/3} f_1(y) \right) E_n^{-1}(y) R_+^{-1}(y) R_+(x) E_n(x) \\ &\quad \times \Psi_+ \left( n^{2/3} f_1(x) \right) \begin{pmatrix} 1 \\ 0 \\ 1 \\ 0 \end{pmatrix}. \end{aligned} \quad (5.6)$$

The term  $e^{n\operatorname{Re}(\lambda_{4+}(y) - \lambda_{1+}(y))}$  is exponentially small, and does not contribute to the limit. Then we can use the arguments of [6, section 9.3] to obtain (2.11). Similar arguments give (2.11) in case  $u > 0$  and/or  $v > 0$ .

Likewise we get (2.12).

## 6 Steepest descent analysis and proofs of theorems for case $t_{c,1} < t < t_{c,2}$

The steepest descent analysis is somewhat different for the case  $t_{c,1} < t < t_{c,2}$ , due to the different sheet structure of the Riemann surface, see Figure 7. However the main lines in the proof remain the same. We only point out that now we have two pairs of purely imaginary branch points,  $\pm iz_2$  and  $\pm iz_3$ . In the second transformation we need to open two global lenses in order to remove the exponentially increasing entries in the jump matrices. After the small opening of a lens around  $(-z_1, z_1)$  we then construct local parametrices at the branch points with Airy functions.

At the end of the transformations we arrive at a RH problem for  $R$  with jumps on the contour shown in Figure 16. The jump conditions for  $R$  are  $R_+ = R_-(I + O(1/n))$ , uniformly on all parts of the contour. Then similar arguments and calculations lead to the proofs of Theorems 2.1–2.3 for the case  $t_{c,1} < t < t_{c,2}$ . We refer to [11] for complete details.

## References

- [1] M. Adler and P. van Moerbeke, PDE's for the Gaussian ensemble with external source and the Pearcey distribution, preprint math.PR/0509047, to appear in Comm. Pure Appl. Math.
- [2] M. Adler and P. van Moerbeke, Joint probability for the Pearcey process, preprint math.PR/0612393.

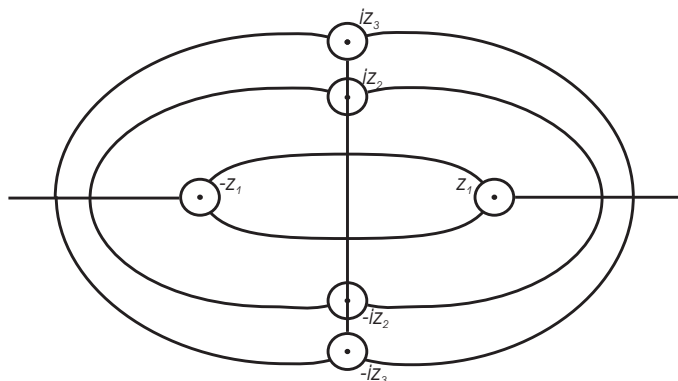


Figure 16: Jump contour for the RH problem for  $R$  in case  $t_{c,1} < t < t_{c,2}$  and  $t \neq a/(a+b)$  (for  $t = a/(a+b)$  we have  $z_2 = z_3$  and then we can simplify the contour by letting the two global lenses coincide). The  $4 \times 4$  matrix valued function  $R$  is analytic outside these contours, and has jumps  $R_+ = R_-(I + O(1/n))$  uniformly on all parts of the contour.

- [3] M. Adler, P. van Moerbeke, and P. Vanhaecke, Moment matrices and multi-component KP, with applications to random matrix theory, preprint math-ph/0612064.
- [4] A.I. Aptekarev, P.M. Bleher, and A.B.J. Kuijlaars, Large  $n$  limit of Gaussian random matrices with external source, part II, *Comm. Math. Phys.* 259 (2005), 367–389.
- [5] P.M. Bleher and A.B.J. Kuijlaars, Random matrices with external source and multiple orthogonal polynomials, *Int. Math. Research Notices* 2004, no 3 (2004), 109-129.
- [6] P.M. Bleher and A.B.J. Kuijlaars, Large  $n$  limit of Gaussian random matrices with external source, part I, *Comm. Math. Phys.* 252 (2004), 43-76.
- [7] P.M. Bleher and A.B.J. Kuijlaars, Large  $n$  limit of Gaussian random matrices with external source, part III: double scaling limit, *Comm. Math. Phys.* 270 (2007), 481–517
- [8] A. Borodin, Biorthogonal ensembles, *Nucl. Phys. B* 536 (1998), 704–732.
- [9] E. Brézin and S. Hikami, Universal singularity at the closure of the gap in a random matrix theory, *Phys. Rev. E* 57 (1998), 4140–4149.
- [10] E. Brézin and S. Hikami, Level spacing of random matrices in an external source, *Phys. Rev. E* 58 (1998), 7176–7185.

- [11] E. Daems, Asymptotics for non-intersecting Brownian motions using multiple orthogonal polynomials, Ph.D. thesis, K.U.Leuven, 2006, URL <http://hdl.handle.net/1979/324>.
- [12] E. Daems and A.B.J. Kuijlaars, A Christoffel Darboux formula for multiple orthogonal polynomials, *J. Approx. Theory* 130 (2004), 188-200.
- [13] E. Daems and A.B.J. Kuijlaars, Multiple orthogonal polynomials of mixed type and non-intersecting Brownian motions, preprint math.CA/0511470, to appear in *J. Approx. Theory*.
- [14] P. Deift, *Orthogonal Polynomials and Random Matrices: a Riemann-Hilbert approach*. Courant Lecture Notes in Mathematics Vol. 3, Amer. Math. Soc., Providence R.I. 1999.
- [15] P. Deift, T. Kriecherbauer, K.T-R McLaughlin, S. Venakides, and X. Zhou, Uniform asymptotics for polynomials orthogonal with respect to varying exponential weights and applications to universality questions in random matrix theory, *Comm. Pure Appl. Math.* 52 (1999), 1335–1425.
- [16] P. Deift, T. Kriecherbauer, K.T-R McLaughlin, S. Venakides, and X. Zhou, Strong asymptotics of orthogonal polynomials with respect to exponential weights, *Comm. Pure Appl. Math.* 52 (1999), 1491–1552.
- [17] P. Desrosiers and P. Forrester, A note on biorthogonal ensembles, preprint math-ph/0608052.
- [18] F.J. Dyson, A Brownian-motion model for the eigenvalues of a random matrix, *J. Math. Phys.* 3 (1962), 1191–1198.
- [19] A.S. Fokas, A.R. Its, and A.V. Kitaev, The isomonodromy approach to matrix models in 2D quantum gravity, *Commun. Math. Phys.* 147 (1992), 395–430.
- [20] K. Johansson, Non-intersecting paths, random tilings and random matrices, *Probab. Theory Related Fields* 123 (2002), 225–280.
- [21] S. Karlin and J. McGregor, Coincidence probabilities, *Pacific J. Math.*, 9 (1959), 1141–1164.
- [22] A.B.J. Kuijlaars, Riemann-Hilbert analysis for orthogonal polynomials. In: *Orthogonal Polynomials and Special Functions* (E. Koelink and W. Van Assche eds.), *Lecture Notes in Math.*, 1817, Springer, Berlin, pp. 167–210.
- [23] A.B.J. Kuijlaars, W. Van Assche, and F. Wielonsky, Quadratic Hermite-Padé approximation to the exponential function: a Riemann-Hilbert approach, *Constr. Approx.* 21 (2005), 351–412.

- [24] R. Miranda, Algebraic Curves and Riemann Surfaces, American Mathematical Society, Providence, RI, 1995.
- [25] A. Okounkov and N. Reshetikhin, Random skew plane partitions and the Pearcey process, *Comm. Math. Phys.* 269 (2007), 571–609.
- [26] V. Lysov and F. Wielonsky, Strong asymptotics for multiple Laguerre polynomials, to appear in *Constr. Approx.*
- [27] M.L. Mehta, Random Matrices, 2nd edition, Academic Press, Boston, 1991.
- [28] A. Soshnikov, Determinantal random point fields, *Russian Mathematical Surveys* 55 (2000), 923–975.
- [29] C. Tracy and H. Widom, The Pearcey process, *Comm. Math. Phys.* 263 (2006), 381–400.
- [30] C. Tracy and H. Widom, Non-intersecting Brownian excursions, preprint math.PR/0607321.
- [31] W. Van Assche, J.S. Geronimo and A.B.J. Kuijlaars, Riemann-Hilbert problems for multiple orthogonal polynomials, *Special Functions 2000: Current Perspectives and Future Directions* (J. Bustoz et al., eds.), Kluwer, Dordrecht, 2001, pp. 23–59.